Climate Risk Management 54 (2026) 100893

Contents lists available at ScienceDirect

Climate Risk Management

journal homepage: www.elsevier.com/locate/crm

Urban pluvial flood risk mapping: a high-resolution assessment for the city of Hamburg

Malte von Szombathely [a,*], Jörn Behrens [b], Franziska Stefanie Hanf [c,d], Marc Lennartz [e], Shefali Nayak [f], Jürgen Oßenbrügge [g], Benjamin Poschlod [a,h], Jürgen Scheffran [g], Anastasia Vogelbacher [g], Jana Sillmann [a,i]

[a] Research Unit Sustainability and Climate Risk, and Earth and Society Research Hub (ESRAH), Universität Hamburg, Grindelberg 5, 20144 Hamburg, Germany
[b] Dept. of Mathematics and Earth and Society Research Hub (ESRAH), Universität Hamburg, Grindelberg 5, 20144 Hamburg, Germany
[c] Systemic Risks, Research Institute for Sustainability (RIFS) at GFZ Helmholtz Centre for Geosciences, Berliner Straße 130, 14467 Potsdam, Germany
[d] Meteorology, Department of Earth System Sciences, Faculty of Mathematics, Informatics and Natural Sciences, Earth and Society Research Hub (ESRAH), Universität Hamburg, Bundesstr. 55, 20146 Hamburg, Germany
[e] Section Hydrology, GFZ Helmholtz Centre for Geosciences, P.O. Box 60 12 03, 14412 Potsdam, Germany
[f] HafenCity University Hamburg, University of the Built Environment and Metropolitan Development, Henning-Voscherau-Platz 1, 20457 Hamburg, Germany
[g] Geography, Earth and Society Research Hub (ESRAH), Universität Hamburg, Bundesstr. 57, 20146 Hamburg, Germany
[h] Institute for Global Water Security, Hamburg University of Technology, Harburger Schloßstraße 22a, 21079 Hamburg, Germany
[i] Center for International Climate and Environmental Research (CICERO), Oslo, Norway

ARTICLE INFO

Keywords:
Urban flooding
Flood risk
Pluvial flood
Risk mapping
Social vulnerability
High resolution

ABSTRACT

This study develops a high-resolution pluvial flood risk index by integrating hazard modeling, exposure assessment, and social vulnerability analysis following the IPCC risk framework, and applies it to the city of Hamburg, Germany as a case study. The hazard component is based on a 100-year rainfall event (36 mm/h), modeled using a hydrodynamic flood simulation that accounts for topography, drainage capacity, and land use. Exposure differentiates between mobility-related risks and well-being-related risks, while social vulnerability is quantified using socio-economic indicators such as age, income, and education status.

The results highlight risk hotspots where social vulnerability and flood exposure overlap, providing decision-makers with valuable insights for targeted interventions. The study reveals that social vulnerability does not correlate directly with flood hazard, emphasizing the

Abbreviations: AR, Assessment Report; BUKEA, Hamburg's environmental agency (Umwelt, Klima, Energie, Agrarwirtschaft); E, Exposure; E_{MA}, Exposure related to mobility & accessibility; E_{WB}, Exposure related to well-being; FHH, Free and Hanseatic City (Freie und Hansestadt) of Hamburg; H, Hazard; H_{MA}, Hazard to mobility and accessibility; H_{WB}, Hazard to well-being; IPCC, Intergovernmental Panel on Climate Change; MA, Mobility & accessibility; PFR, Pluvial flood risk; PFR_{MA}, Pluvial flood risk to mobility & accessibility; PFR_{WB}, Pluvial flood risk to well-being; SV, Social vulnerability; SV_{PF}, Social vulnerability to pluvial flooding; SVI, Social vulnerability index; TOPSIS, Technique for Order Preference by Similarity to Ideal Solution; WB, Well-being.

* Corresponding author.
E-mail addresses: malte.szombathely@uni-hamburg.de (M. von Szombathely), joern.behrens@uni-hamburg.de (J. Behrens), franziska.stefanie.hanf@rifs-potsdam.de (F.S. Hanf), marc.alexander.lennartz@gfz.de (M. Lennartz), shefali.nayak@hcu-hamburg.de (S. Nayak), juergen.ossenbruegge@uni-hamburg.de (J. Oßenbrügge), benjamin.poschlod@tuhh.de (B. Poschlod), juergen.scheffran@uni-hamburg.de (J. Scheffran), anastasia.vogelbacher@uni-hamburg.de (A. Vogelbacher), jana.sillmann@uni-hamburg.de (J. Sillmann).

https://doi.org/10.1016/j.crm.2026.100893
Received 2 April 2025; Received in revised form 25 September 2026; Accepted 5 October 2026
Available online 7 October 2026
2212-0963/© 2026 The Authors. Published by Elsevier B.V. This is an open access article under the CC BY license (http://creativecommons.org/licenses/by/4.0/).
Open access funding enabled and organized by Projekt DEAL.

complexity of urban flood risk. This underscores the need for a holistic approach to risk assessment, integrating climate science, infrastructure planning, and social policies to enhance urban resilience. The methodology deployed in this study is useful for other urban areas, showing its value for climate change adaptation planning and risk-informed decision-making.

1. Introduction

Cities around the globe are facing increasing challenges due to climate change, which is expected to exacerbate the frequency, severity, and impact of extreme events throughout the 21st century (Lockwood et al., 2024; Rosenzweig et al., 2024; Wu et al., 2024). Among these, pluvial floods have emerged as a significant threat to public health and infrastructure (Schmitt and Scheid, 2020). The intensification of triggering sub-daily rainfall extremes is already diagnosed in the current climate (Guerreiro et al., 2018; Haslinger et al., 2025; Lang and Poschlod, 2024; Poschlod, 2022) and projected to strongly increase under future warming (Fowler et al., 2021; Kendon et al., 2023; Kendon et al., 2018; Marra et al., 2024; Poschlod and Ludwig, 2021; Prein et al., 2017). Pluvial flooding accounts for a substantial proportion of flood impacts, with some countries reporting a ratio of approximately 30% to 50% of all flood-related incidents (Schanze, 2018). Unlike large-scale riverine floods or coastal flooding, urban pluvial floods are often driven by localized rainfall stemming from convective cells, which are challenging for numerical weather forecasting (Judt, 2018; Rözer et al., 2021) and climate modeling. Even though convection-permitting weather and climate models can improve the representation of such small-scale high-intensity events (Chan et al., 2016; Fosser et al., 2024; Fosser et al., 2020; Lind et al., 2023; Poschlod et al., 2018; Poschlod and Koh, 2024), their exact location and time of occurrence is very uncertain due to internal climate variability (Judt, 2018; Lavin-Gullon et al., 2021; Poschlod et al., 2021).

Hence, urban pluvial flooding can occur everywhere and has increasingly become a focal point of concern within the sphere of urban water and flood risk management. Characterized by the inundation resulting from short and intense rainfall that converges in topographical sinks and overwhelms the capacity of natural and engineered drainage systems, urban pluvial flooding poses a significant threat to the infrastructure, economy, and well-being of citizens around the globe (Falconer et al., 2009). Urbanization exacerbates the issue, as the impermeable surfaces of city landscapes limit the infiltration, leading to increased surface runoff and flood risk. This dual catalyst demands an urgent and comprehensive response to enhance flood protection measures. This is a particular challenge in the multi-flood hazard hotspot of Hamburg (Hanf et al., 2025), where the diversity of pluvial, fluvial and coastal flooding requires different flood protection measures, and a combination of flood types can lead to complex and devastating flood scenarios (Guan et al., 2023; Jiang et al., 2024; Rosenzweig et al., 2024; Santos et al., 2021; Wahl et al., 2015). Hamburg recently experienced two severe localized heavy rainfall events (Lohbrügge in 2018; Barmbek in 2024) that caused damage to roads and homes, led to evacuations, and restricted mobility within the neighborhood (compare Deutscher Wetterdienst (DWD), 2021). The urgency to address pluvial flood risks in urban settings is underscored by the necessity to support decision-making in the design of adaptation measures for resilient cities (Fereshtehpour and Najafi, 2025; Hanf et al., 2024; Thieken et al., 2016). Such adaptation planning is not only a matter of infrastructure but requires holistic approaches (Hanf et al., 2025) including a link between climate science, social science, impact science, and decision-makers fostering policy, planning, and community preparedness (Allegri et al., 2024; Rözer et al., 2016; Sillmann et al., 2024). The management of urban pluvial flooding requires sophisticated approaches to hazard mapping and risk assessment. However, despite the clear need for such methodologies, the development of a common framework for pluvial flood hazard mapping and subsequent risk assessment remains elusive (Fritsch et al., 2016), highlighting the need for comprehensive datasets that can strengthen the reliability of available information, potential impact and adaptation measures.

A general approach to assess climate risk used in this study is based on a tripartite conceptual model that includes the complex interaction between climate-related hazard, exposure, and vulnerability following the 6th Assessment Report (AR6) of the Intergovernmental Panel on Climate Change, IPCC (Reisinger et al., 2020). While hazard and exposure are often quantified in flood risk assessments, social vulnerability tends to be inadequately addressed. However, this risk component is of significant importance, as whilst the impacts of hazards themselves cannot be entirely mitigated, the vulnerability of the elements at risk can be reduced (Santos et al., 2026). Social vulnerability is defined as the susceptibility to harm from exposure to a hazard event, stemming from social factors such as education, income inequality, age demographics, and accessibility to essential services (Fox et al., 2024). On a global scale, an empirical social vulnerability map, Global Social Vulnerability Index, was developed recently based on very similar indicators, established through the analysis of past flood fatalities (Reimann et al., 2024), building on existing conceptual considerations and indices (Cutter et al., 2003; Fekete and Rufat, 2023). For Hamburg, a social vulnerability index (SVI) exists (von Szombathely et al., 2023), which also refers to these indicators. These analyses underscore the critical need to incorporate social vulnerability within the flood risk assessment framework to ensure a comprehensive understanding of risk.

This paper aims to dissect the complexity of urban pluvial flooding risk via the analysis of freely available, high-resolution data for the city of Hamburg. It is a city characterized by an overall flat topography with many depressions (rivers, marshlands, old moors). Hamburg has a long history of flooding events, with the tragic storm surge of 1962 as the most significant event (De Guttry and Ratter, 2022), for example, and many pluvial floods in recent years (Bischoff et al., 2021). The primary objective of this study is to present the first city-wide implementation of a high-resolution, building-scale pluvial flood risk assessment framework based on the IPCC risk concept, integrating hazard, exposure, and social vulnerability. Developed in close collaboration with stakeholders from the City of Hamburg, the framework provides a transferable approach for comprehensive urban flood risk assessment and management (Vogelbacher et al., 2026), with the understanding that it must be adapted to city-specific risk characteristics with the help of local

stakeholders. We visualize the city-wide results in an innovative and continuous way, based on smoothed Voronoi cells.

The framework introduces two risk indices, addressing direct risks to well-being as well as restrictions of mobility and accessibility (Vogelbacher et al., 2026). The well-being index accounts for material damage and costly, time-consuming repairs but also people's well-being, including injuries and in extreme cases, fatalities. The mobility and accessibility index reflects limits on entering or leaving buildings as well as disruptions to critical infrastructure.

With the presentation of high-resolution spatial maps, this analysis aids climate adaptation managers and decision-makers to identify hotspots of increased risk and prioritize effective policy measures for urban climate change adaptation.

2. Risk concept

Risk is evaluated at the building level using the frameworks provided by the IPCC in AR5 and AR6. According to this, our approach links vulnerability, exposure, and hazard (Fuchs et al., 2024) to quantify specific risks related to mobility and accessibility as well as well-being during pluvial flooding events.

Initially, the IPCC's approach to risk was fragmented, with inconsistencies across different Working Groups and assessment cycles (Reisinger et al., 2020). However, since the Special Report on Global Warming of 1.5 °C, efforts have been made to harmonize the risk framework across Working Groups, leading to a more coherent and integrated approach, starting with the AR5 (Reisinger et al., 2020).

While hazard, exposure, and vulnerability are critical in assessing the potential impacts of climate change, risk can also arise due to human responses not achieving the intended outcome. These responses are not the focus of this study, but – in line with the IPCC concept - are already part of the modeling of the hazard data. Hazard (here: pluvial flood) refers to the potential occurrence of a natural or human-induced physical event that may cause harm. In the context of pluvial flooding, hazard maps are generated to depict areas likely to experience such events (FHH, BUKEA, 2024). Exposure denotes the presence of people, livelihoods, environmental services, and resources in places that could be adversely affected by the hazard. We will predominantly focus on the presence of people in this study. Finally, vulnerability is the propensity to suffer damage, which is not solely a function of environmental factors but is typically linked with social parameters (Field et al., 2014). In this study, we focus on social vulnerability, following von Szombathely et al. (2023), to specifically investigate the risk to residential populations.

While the relationship between these factors is undisputed, merely superimposing these does not do justice to the complexity of climate-related risks (Fuchs et al., 2024). A holistic approach is crucial for addressing the multifaceted nature of climate change impacts on both natural and human systems (Marbaix et al., 2025). Several studies rely on the straightforward multiplication of these three sub-indices to define flood risk (Dewan, 2013; Kron, 2005; Veleda et al., 2017; Yang et al., 2018b). While our approach broadly follows this method, we introduce a more sophisticated combination of exposure and hazard by associating a specific group of exposed residents (see Section 4.2) to a specific hazard index (see Section 4.3), building on previous work for accessing vulnerability (von Szombathely et al., 2023).

Fig. 1 outlines our comprehensive framework for flood risk assessment, integrating social vulnerability to floods, exposure, and hazard, discussed in detail in the following chapters. The final risk indices – related to mobility and accessibility and well-being – are calculated by combining social vulnerability (categorized into sensitivity and coping capacity), population exposure, and flood hazard level at the building scale. All three sub-components are designed to have the same weight in the final risk calculation. However, both risk indices differ in the conceptualization of exposure and hazard (see Section 3). This approach provides a detailed and scalable method for evaluating flood-related risks, transferable to other cities worldwide.

3. Data sets

This section discusses the characteristics and sources of the datasets we use to capture aspects of social vulnerability, exposure, and hazard for the city of Hamburg. While the risk framework (Figs. 1 and 3) is applicable across a wide range of cities, the datasets are city-specific and context dependent.

3.1. Social vulnerability: socio-economic data

The demographic and socio-economic data for the city of Hamburg is available at the resolution of so-called statistical units, which split Hamburg into 943 sub-regions (status: December 2023), see Fig. 2 (FHH, Statistikamt Nord, 2024; Maaß et al., 2023). The statistical units are conceptualized as a grouping of neighboring building blocks that are assumed to be homogeneous in terms of their building and socio-structural characteristics (FHH, Statistikamt Nord, 2017). For our analysis we use the number of children under 10 years old, singles over 65 years old, people without a high school diploma and receivers of social welfare, and calculate the relative share of these four indicators in the total number of inhabitants per statistical unit. Statistical areas with less than 300 inhabitants are excluded in the social monitoring by the city authorities (Maaß et al., 2023; Maaß and Huang, 2024) due to privacy concerns in sparsely populated areas. Therefore, in some of these areas, the necessary subgroups are not available. However, in the pre-processing of the input data, we employ the available Population data and means across Hamburg to calculate risk for as many inhabited buildings as possible, in order to identify high-risk buildings, particularly in peripheral locations.

3.2. Exposure: buildings and streets data

The data on the number of inhabitants comes from the same data set as for social vulnerability (FHH, Statistikamt Nord, 2024). The

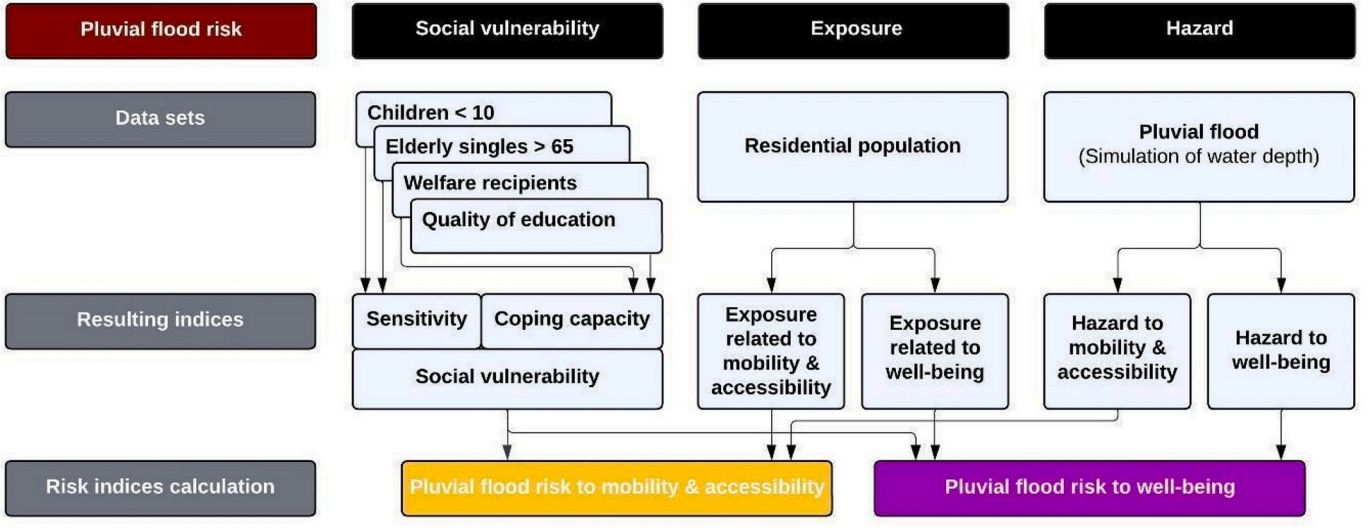


Fig. 1. Basic structure of Pluvial Flood Risk Assessment. Methodological process for assessing flood-related risks, integrating social vulnerability, exposure, and hazard components into a unified evaluation model, based on Reisinger et al. (2020).

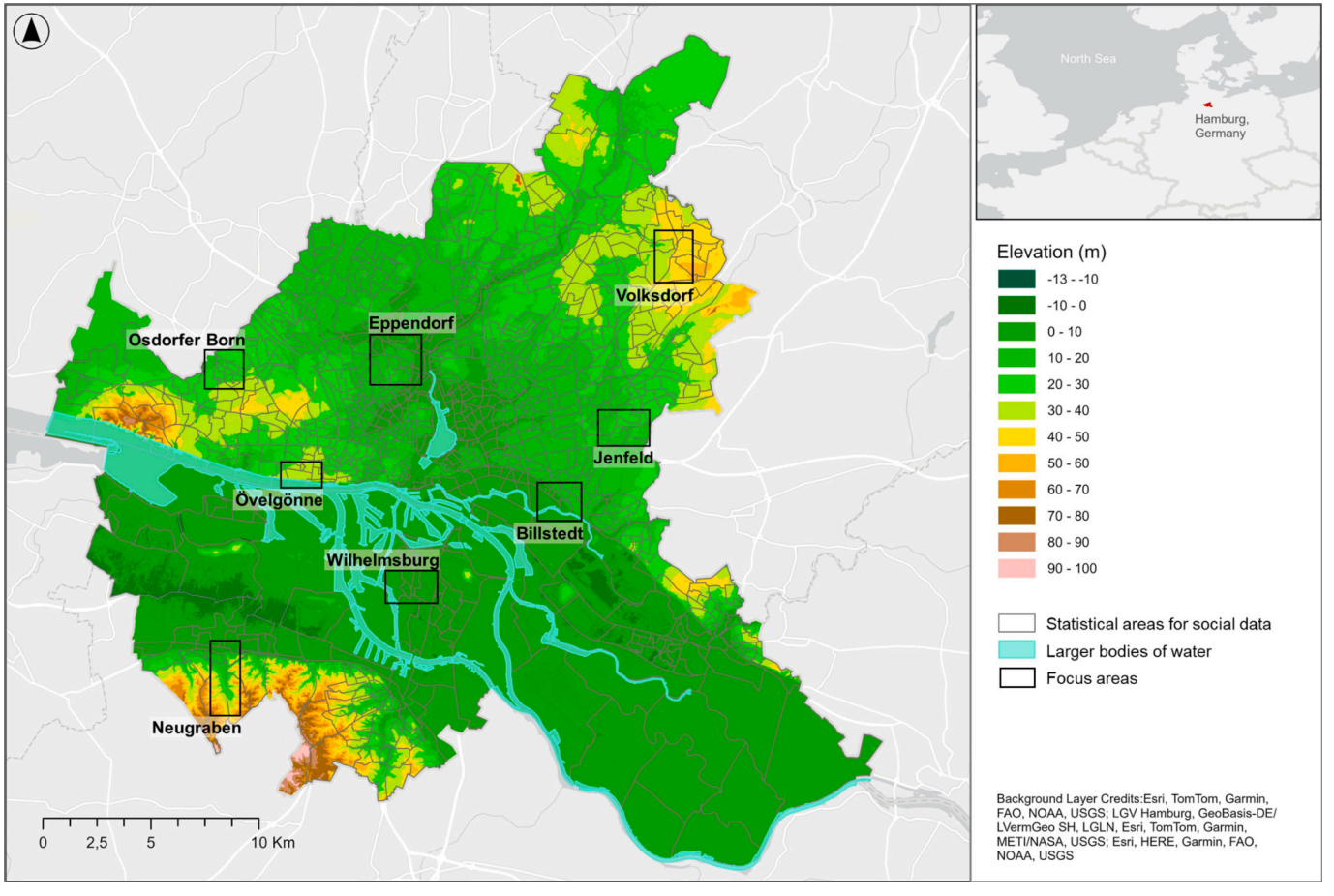


Fig. 2. Topographical overview of the study area. Grey outlines mark statistical areas (resolution of social data for social vulnerability and exposure). Black squares highlight focus areas within Hamburg, across all figures.

geodata required for our spatial analysis are the road and the building outlines. Both are taken from the official land register information system (ALKIS) dataset which is provided by the city of Hamburg (FHH, LGV, 2017, 2020). The road dataset has been recorded in April 2019, whereas the building data is from July 2020.

3.3. Hazard: modeled flood level data

The simulations of pluvial flooding are provided by Hamburg's water supply and wastewater disposal company HAMBURG WASSER on behalf of and in cooperation with the Hamburg Ministry for Environment, Climate, Energy and Agriculture (BUKEA). The modeled data is freely available online via the Geoportal Hamburg (FHH, BUKEA, 2024). The pluvial flood assessment is based on hydrodynamic model simulations that consider precipitation intensity, surface runoff, infiltration capacity into the ground, interception and the capacity of the public sewer system. The 2-dimensional numerical surface runoff model framework VISDOM (Blöschl et al., 2024; Buttinger-Kreuzhuber et al., 2019, 2022a, 2022b; Waser et al., 2011) is bi-directionally coupled with the 1-dimensional numerical Storm Water Management Model (Rossman and Simon, 2022) representing the sewer system. The simulations are carried out on the basis of a digital terrain model at 1-m resolution considering retention basins and ditches. We select the pluvial flood scenario triggered by a design rainfall of 36 mm/h reflecting a 100-year event (FHH, BUKEA, 2024).

4. Methodology

All assumptions and procedures applied in this framework are described here. In addition,we refer to Vogelbacher et al., 2026), where the development and underlying assumptions of the applied methodology is described in detail. The prerequisite for this combination of social vulnerability, exposure and hazard is high-resolution data (see also Section 3). We are convinced of the fundamental transferability of this approach to other risk analyses, therefore we emphasize the importance of transparent data availability.

4.1. Social vulnerability

von Szombathely et al. (2023) propose a social vulnerability index for Hamburg, which is tailored to flood hazards. Four specific socio-economic variables are identified that contribute to increased vulnerability in urban areas and enable the calculation of a social vulnerability index (SVI), divided into *sensitivity* and *coping capacity*. *Sensitivity* is the extent to which a system is influenced (negatively or positively), while *coping capacity* refers to the way in which people make use of available resources. Income disparity and educational attainment are used to calculate *coping capacity*, while the proportions of children and old single inhabitants reflect *sensitivity*.

By employing spatial analysis, the concept of von Szombathely et al. (2023) is able to identify neighborhoods that are disproportionately affected by these socio-economic challenges. For Hamburg as a whole the proportion of children and old single inhabitants in each statistical area is almost normally distributed. They have a mean value of ~9% and ~ 7%, respectively, with a standard deviation of 2.8% for both. On the other hand, the proportion of people receiving social welfare and people without a high school diploma are distributed similarly to an exponential decay function. These variables have a mean of 7% and 1%, as well as a standard deviation of 8.5% and 0.8% respectively.

von Szombathely et al. (2023) apply weights (based on expert knowledge) on the indicators reflecting income, education, and age, which originate from the use of an analytic hierarchy process, AHP (Saaty, 1990). These weights reflect the relative importance of each variable in assessing vulnerability (see Table 1). We modify the index by von Szombathely et al. (2023) emphasizing the importance of heterogeneity of indicators within the city, following Yang et al., 2018b. They argue that the inhomogeneity of the indicators is an important feature influencing the flood vulnerability of an area (compare Vogelbacher et al., 2026).

Therefore, within the calculation of *sensitivity* and *coping capacity*, we apply the Technique for Order Preference by Similarity to Ideal Solution, TOPSIS (Hwang and Yoon, 1981) and the Shannon entropy (Shannon, 1948). TOPSIS is a ranking method assessing the shortest distance from the positive ideal solution and the farthest distance from the negative ideal solution in a multi-dimensional space (Yang et al., 2018b). The method includes a normalization and a weighted combination of variables into one index. The weights of variables are determined in advance using the analytic hierarchy process, as outlined above. The combination of the analytic hierarchy process and TOPSIS is widely applied in the context of flood related vulnerability analyses (Vogelbacher et al., 2026; Boultif and Hafnaoui, 2026; Ekmekcioğlu et al., 2021; Nguyen et al., 2020; Pathan et al., 2022; Rafiei-Sardooi et al., 2021; Yang et al., 2018b).

Additionally, we argue that inhomogeneity in the normalized and weighted values of the different indicators of a component will influence the flood vulnerability. The Shannon entropy method is chosen to quantify the inhomogeneity of all social vulnerability variables within the city. Conceptually we follow the rationale of Yang et al. (2018b); noticeably, we do not use the Shannon entropy method to find the “objective weight” of the social indicators (e.g., compare Ji and Wang, 2023). Subsequently, the integrated social vulnerability index is derived by reapplying TOPSIS and Shannon entropy to the two components, *sensitivity* and *coping capacity*. Note that the weights applied are based on the available social variables and should be reevaluated for different case studies (compare Vogelbacher et al., 2026).

The resulting SVI considers the combined effect of both the total social vulnerability score and the internal inhomogeneity of the indicators. The analysis focuses on statistical units but may also be performed at the building resolution if the data is available.

The SVI considers the relative distances of the social parameters and their heterogeneity. That means that the vulnerability index follows a probability distribution similar to the distribution of the social-economic indicators. However, we do not assume that flood

Table 1
Overview of data and calculations.

Dimensions of risk	Datasets used	Original resolution	Weights	Calculations	Outputs	Output resolution
Social Vulnerability	Number of children <10 years old (C) Elderly singles >65 years old (ES) People without high school diploma, last 3 years (EDQ) Receivers of social welfare (WR)	Statistical unit	0,3 0,7 0,5 0,5	TOPSIS & Shannon Entrophy, + ¼ SD & squaring, linear disaggre- gation	SV_{PF}	Building
Exposure	Residents per building (R) and residents per ground floor level (RG) Nr. of floors above ground and building type/function	Statistical unit Building level		Linear disaggre- gation based on living space	E_{MA}, E_{WB}	Building
Hazard	Water level based on pluvial flood scenario with a rainfall of 36 mm/h reflecting a 100-year event Street outlines	1 m^2 1 m		Intersected areas with flood layers > 30 cm, damage function	H_{MA}, H_{WB}	Building

risk scales linearly with the SVI. Hence, an additional transformation is necessary which reflects the relationship of flood vulnerability between groups with average SVI and very high SVI values. We place an additional emphasis in the most vulnerable groups by squaring the SVI. This is a subjective choice based on expert knowledge, which has been shown to be more accurate than statistical models in assessing flood related social vulnerability (Rufat et al., 2019). Additionally, the SVI is a complex latent variable, and our choice of observable socio-economic variables is limited. Thus, there may be data samples showing an SVI value of zero or near-zero. In our framework, where risk is a product of hazard, exposure and vulnerability, this assumption would lead to zero or near-zero risk values even with high exposure and high hazard indices. In response, we add a minimum threshold to all SVI values, defined to be a quarter of the distance between 0 and the mean of the SVI. The value of this threshold is a normative choice which depends on the shape of the SVI distribution, which is in turn governed by the number of social-economic indicators among others. With the transformation and addition of the minimum threshold, we turn the generic SVI into the context-specific *social vulnerability to pluvial flooding* (SV_{PF}), placing more emphasis on extreme values and extreme heterogeneity in a statistical area, thus helping to identify actual 'hotspots' of increased risk.

4.2. Exposure

In accordance with the IPCC concept, for exposure we consider the *presence of people* in places that could be adversely affected. For this study, these are the inhabitants of the city of Hamburg in relation to their places of residence. Since the selected hazard can have very different effects (Hammond et al., 2015; He et al., 2023; Lamond et al., 2015; Van Ootegem et al., 2015), possible risk outcomes had to be defined first, which could then be related to different concepts of exposure. In connection with exposure to flash floods, we have decided to examine two different concepts: We distinguish between mobility restrictions and reduction in well-being. This inevitably results in two different exposure concepts, as there are different hazard types for each building and different groups of people may be affected.

For restrictions of mobility and accessibility we consider all people in the respective building (E_{MA}, exposure related to mobility & accessibility), and for danger to well-being and property only people from the ground floor are to be considered (E_{WB}, exposure related to well-being, see Table 1 and Fig. 3).

Due to data protection regulations, the number of residents in each residential building is not publicly accessible. Population data is available at the resolution of statistical units. The building data set provides detailed information about each building, including the number of floors above ground and the building's primary function. The buildings may serve as either fully residential or mixed-use, incorporating residential purposes alongside other functions.

Assuming a homogeneous population density within one statistical unit, we distribute the population of a statistical unit to all residential buildings within the area weighted by the living space of each building. For buildings classified as "mixed use", we assume that the first floor is used for commercial purposes and does not contribute to living space. This approach ensures a more precise allocation of population data across individual buildings, enhancing the spatial resolution and accuracy of our assessment.

4.3. Hazard

The pluvial flood hazard data (simulation data of the city of Hamburg, see above) has a native resolution of 1 square meter, allowing for detailed spatial assessments. We define water level thresholds based on existing studies on pluvial floods (Bhola et al., 2020; Calianno et al., 2013; Lazzarin et al., 2022) and building regulations (Bignami, 2019; Rose and Wilke, 2015), setting 30 cm water depth as the basic threshold value. Thus we arrive at two different hazard indices, each of which depicts different pluvial flood hazards.

For the hazard to mobility and accessibility (H_{MA}) a threshold for flooding near buildings of 30 cm is used, assessing how flooding impacts movement and access in affected areas. For the hazard to one's well-being (H_{WB}) all water levels between 30 cm to over 1 m are used, with water being present directly at buildings (see Fig. 3), evaluating the potential for damage and danger to well-being. These two dimensions of the hazard are developed alongside the two dimensions of exposure and are closely interconnected with it (see Table 1 and Fig. 3).

4.3.1. Hazard affecting the well-being of inhabitants

We devise a 2-m buffer around all buildings, reflecting the potential intrusion of water due to the elevated water level near the building (see Vogelbacher et al., 2026 for details). Within this buffer zone, we assess a range of water levels (30 cm to 1 m, in increments of 10 cm) to capture varying levels of potential impact (see Vogelbacher et al., 2026 for details).

The hazard index related to well-being (H_{WB}) is calculated as follows:

For the cumulative distribution function (CDF) of the log-normal distribution

$$F_X(x) = \Phi\left(\frac{ln\,(x) - \mu}{\sigma}\right), \tag{1}$$

we choose $\mu = 0$ and $\sigma = 0.25$, with Φ as the CDF of the standard normal distribution. We derive the hazard index

$$H_{WB} = \sum_{i=30}^{100} \left[F_X\left(4 \cdot A_{2m,i}\right)\right], \quad i \in \{30, 40, 50, 60, 70, 80, 90, 100\}, \tag{2}$$

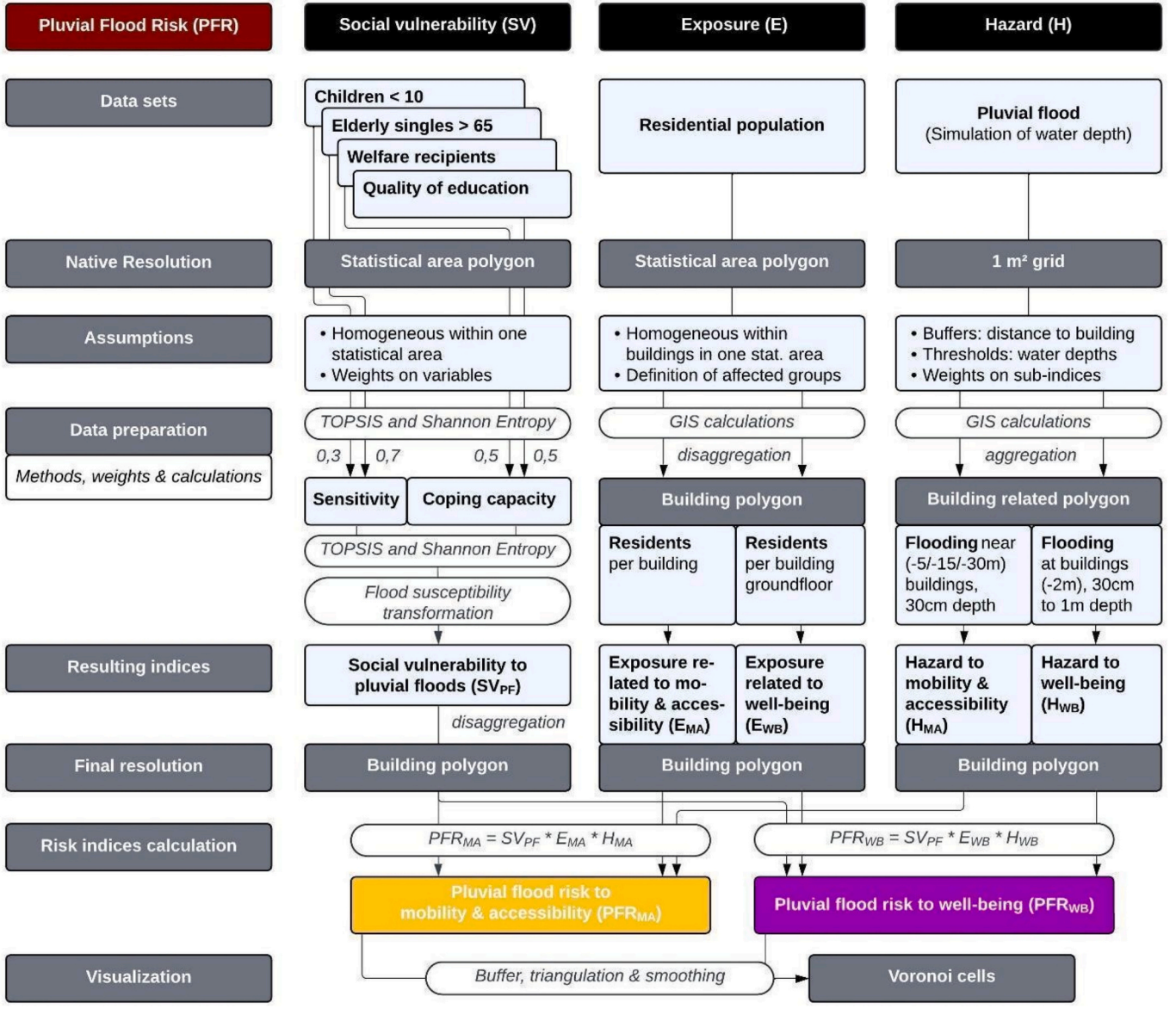


Fig. 3. Detailed framework and components of Pluvial Flood Risk Assessment. Detailed processes for assessing flood-related risks to well-being and mobility & accessibility, integrating social vulnerability, exposure, and hazard components.

with $A_{2m,i}$ as the fraction of the flooded area within a 2 m buffer at the water level i (in centimeter).

4.3.2. Hazard affecting the mobility and accessibility of inhabitants

We employ buffers of 5, 15, and 15-to-30 m around an affected building. The 5-m buffer indicates the feasibility of entering and leaving the building, while the 15-m and 15-to-30-m buffers consider intersections with the road network. The two latter buffers collectively assess whether vehicular access to the building is possible during flooding (see Vogelbacher et al., 2026 for details).

The hazard index related to mobility and accessibility (H_{MA}) is calculated using the maximum value derived from the following equation:

$$H_{MA} = \left[F_X\left(4 \cdot A_{5m,30cm}\right), F_X\left(4 \cdot R_{15m,30cm}\right), F_X\left(4 \cdot R_{30m,30cm}\right)\right]. \tag{3}$$

There, $A_{5m,30cm}$ refers to the fraction of area within a 5 m buffer, which is flooded above a 30 cm water level. $R_{15m,30cm}$ and $R_{30m,30cm}$ describe the fraction of road area within a 15 m buffer and 15-to-30 m buffer, respectively, which are flooded above a 30 cm water level.

4.4. Risk

Building on the above-mentioned sub-indices for social vulnerability, exposure and hazard, we assess risk at the building level in this study. Our approach now links vulnerability, exposure, and hazard to quantify two specific risks during pluvial flooding events, one related to mobility and accessibility and the other related well-being.

The index of **pluvial flood risk to mobility & accessibility (PFR_{MA})** metric is calculated as:

$$PFR_{MA} = SV_{PF} \cdot E_{MA} \cdot H_{MA}. \tag{4}$$

Here, the mobility and accessibility hazard parameter (H_{MA}) quantifies the restriction of the building accessibility during flooding, while the *residents per building* parameter (E_{MA}) accounts for the number of individuals dependent on this access. The social vulnerability to floods (SV_{PF}) at the building level captures the socio-economic attributes (see Section 4.1). The index of **pluvial flood risk to well-being (PFR_{WB})** metric is calculated as:

$$PFR_{WB} = SV_{PF} \cdot E_{WB} \cdot H_{WB}. \tag{5}$$

In this case, the H_{WB} represents the potential intrusion of floodwater into the building, particularly at the ground floor level, which is most exposed to direct flood impacts. The number of *residents on the ground floor per building* (E_{WB}) is a critical factor, as these individuals are at the highest risk of physical harm or property damage. The inclusion of SV_{PF} highlights the role of social indicators in determining the extent to which health outcomes are impacted during flooding.

These calculations ensure that risk assessments are both granular and context-sensitive, addressing the specific concepts of exposure for different models of the hazard pluvial flood. This methodology provides a comprehensive evaluation of flood-related risks at the building level, aligning with the IPCC's multidimensional framework for risk assessment.

4.5. Visualization

Publishing high-resolution results at the building level is problematic for two reasons: First, the final risk index values do not sufficiently reflect the possible sources of uncertainty associated with the numerous input data. Second, it is possible that high-resolution risk data may have negative consequences for homeowners (e.g. increased insurance premiums).

After intensive internal discussions and consultation of stakeholders on these matters, we applied a smoothing function to the results to avoid publishing exact risk values for individual buildings. This makes it difficult to draw conclusions about risks of specific buildings while enabling the identification of risk hotspots at the city-wide scale. At the same time, the smoothing process is accompanied by a more pronounced emergence of risk hotspots (e.g., clusters of houses along a street). Yet, a comparison of the SRI7 scenario analyzed here with the extreme SRI12 (representing a rainfall of 100 mm/h) scenario shows that the hotspots are not artifacts of the smoothing process, but occur consistently even in the event of extreme flash flooding (see S4–6 in supplements).

Thus, the visualization process for a Hamburg-wide map aims at the aggregation of the resolution at building level described above. First, we identify the central point of each building polygon, which serves as a reference for further spatial calculations. Then, we apply the Delaunay-Triangulation on the whole set of building centroids to derive Voronoi cells (Delaunay, 1934; Usui et al., 2020). Thereby, the connecting points between neighboring buildings are determined, ensuring that each building is linked to its nearest neighbors in a structured network. This serves to find a set of neighboring cells over which a smoothing algorithm is performed.

For a given building, the influences of its n neighbors are incorporated to update its attribute value using the following equation:

$$F_{new}(x) = \left(F_{old}(x) + \frac{\sum_{i=1}^{n} \frac{F(i)}{|x-i|}}{\sum_{i=1}^{n} \frac{1}{|x-i|}}\right) \cdot \frac{1}{n+1}, \tag{6}$$

where $F_{old}(x)$ represents the current value associated with the building. $F(i)$refers to the value of a neighboring building i. The term $|x - i|$ denotes the distance between the central points of the building and its neighbor and n is the total number of neighboring

buildings.

This equation ensures that the new value of a building is influenced by the weighted average of its neighbors, where the weights are inversely proportional to the distance between buildings. Additionally, the factor $\frac{1}{n+1}$ normalizes the result, incorporating both the original value of the building and its neighbors' contributions. This smoothing function may be applied several times. For our purpose applying it three times yields the desired fuzziness so that it is no longer possible to draw conclusions about individual buildings. Lastly, to make the visualization of the risk values more intuitive we limit the Voronoi cells to the immediate vicinity of the corresponding building. If no adjacent buildings limit the cell size, a buffer of 100 m (center of the building) is applied.

Classification of the pluvial flood risk indices is carried out using the head/tail break method (Jiang, 2013). This method was developed to categorize value distributions with heavy tails. Class boundaries are defined by calculating the mean and splitting the data into two classes above and below the mean. Afterwards the mean of the upper class is determined, which splits the class in two yet again. This process is repeated iteratively several times. Due to the high resolution the risk distribution is naturally heavy-tailed. In this context the head/tail break method has proven to provide a meaningful classification (Fariza et al., 2015).

5. Results and discussion

5.1. Description of pluvial flood risk patterns

The spatial distribution of pluvial flood risk related to well-being (PFR_{WB}) and risk related to mobility and accessibility (PFR_{MA}) in the study area are visualized in Fig. 4. Areas of high and low risk are scattered across the city, both north and south of the Elbe river. This clearly shows that a pluvial flood and the associated risk can in principle occur anywhere in Hamburg. Even though PFR_{WB} and PFR_{MA} show a positive correlation (Lee's $L = 0.1032$, $p < 0.01$) there is only a partial overlap between PFR_{WB} and PFR_{MA}. As both risk indices are spatially autocorrelated (Moran's I z-scores 116 and 100) we used Lee's L test, developed for autocorrelated variables specifically. While some areas with high risk related to well-being also show mobility-related risks, others exhibit a decoupling effect (see Section 5.2). Overall, larger areas are affected by PFR_{MA} than by PFR_{WB} due to the larger buffers applied (see Eqs. 2 and 3).

The combined risk assessment, visualized in Fig. 4, integrates PFR_{WB} and PFR_{MA} into a single overlay (maps for individual risk indices in supplement, see Figs. S1 and S2). This visualization reveals areas where both types of risks coincide, highlighting neighborhoods with compounding vulnerabilities (Rosenzweig et al., 2024). Notably, the overlap of these two dimensions of risk identifies specific neighborhoods as critical hotspots that require climate change adaptation. We find hotspots of compound high PFR_{WB} and PFR_{MA} (Eppendorf, Billstedt, Övelgönne, Wilhelmsburg, Neugraben) exhibiting both high well-being related risks and severe mobility constraints. These areas may require an integrated approach in adaptation planning, incorporating both flood-resilient urban design and enhanced mobility contingency strategies. Two neighborhoods (Jenfeld and Osdorfer Born), only show high PFR_{MA} values, while PFR_{WB} is low (see Fig. 4 and Section 6). Fig. 4 also reveals a few PFR_{WB} hotspots colored in turquoise and blue. These small areas are characterized by buildings with many inhabitants (on the first floor), buildings where the water is right next to the house, and buildings whose residents are particularly vulnerable to the hazard described.

The spatial pattern of the smoothed PFR_{WB} and PFR_{MA} values for Hamburg shows characteristics that are not comparable with existing socio-economic, topographical or urban morphological analyses. The indices clearly show that the terrain provides only very limited information about the possible effects on a small-scale area (compare Figs. 2 and 4) We highlight one example, where the topography governs the flood risk, however. Areas of high risk are clearly recognizable along one street in Neugraben. The street is located both in a small valley and next to a moat. The street and the adjacent buildings have already been flooded by a heavy rainfall event. The city of Hamburg subsequently commissioned a research project to investigate the specific situation on site (Bischoff et al., 2021). Apart from this example, we find that small-scale conditions on the building level govern the occurrence of high-risk values.

5.2. Relation of pluvial flood risk to social vulnerability indicators and exposure

Fig. 5 shows how the spatial patterns of social vulnerability and the resulting pluvial flood risk indices overlap. Across the city of Hamburg, there is a very low and non-significant correlation between SV_{PF} and H_{MA} (Lee's $L = -0.0020$, $p = 0.536$) as well as SV_{PF} and H_{WB} (Lee's $L = 0.0022$, $p = 0.396$), indicating that the potential occurrence of pluvial flooding has not affected the spatial urban social structure. This distinguishes pluvial floods from storm surges, whose potential flooded areas have affected urban social structures over the past centuries, with socially weaker people living in inundated areas (e.g. Wilhelmsburg; see Fig. 5). Situated in a low-lying floodplain, Wilhelmsburg faces multiple flood risks, including storm surges and fluvial flooding, in addition to pluvial flooding, see Fig. 5 (Abebe et al., 2020; Restemeyer et al., 2015). The district's susceptibility is amplified by its relatively high population density (see Fig. S3) and socio-economic disadvantages, making it a prime example of compounding flood risks. Limited evacuation routes further exacerbate mobility-related challenges (Durst et al., 2014). As a result, this area requires an integrated adaptation approach that combines flood mitigation measures, improved mobility resilience, and targeted social support systems.

The area of Neugraben shows a high flood risk due to exposure and vulnerability factors (e.g. elderly population, flood-prone residential areas) and high hazard values. While mobility-related risks are lower compared to well-being risks, many areas still exhibit notable accessibility challenges. Consequently, the combination of these factors shifts the overall risk profile from pink (PFR_{WB}-dominant) to brownish-red (combined risk to well-being and mobility/accessibility).

A more detailed analysis of the drivers of high vulnerability offers the opportunity to see which specific socio-economic problems need to be accounted for in risk hotspots (Fig. 6). The interaction between SV_{PF} and the hazard is particularly evident in neighborhoods

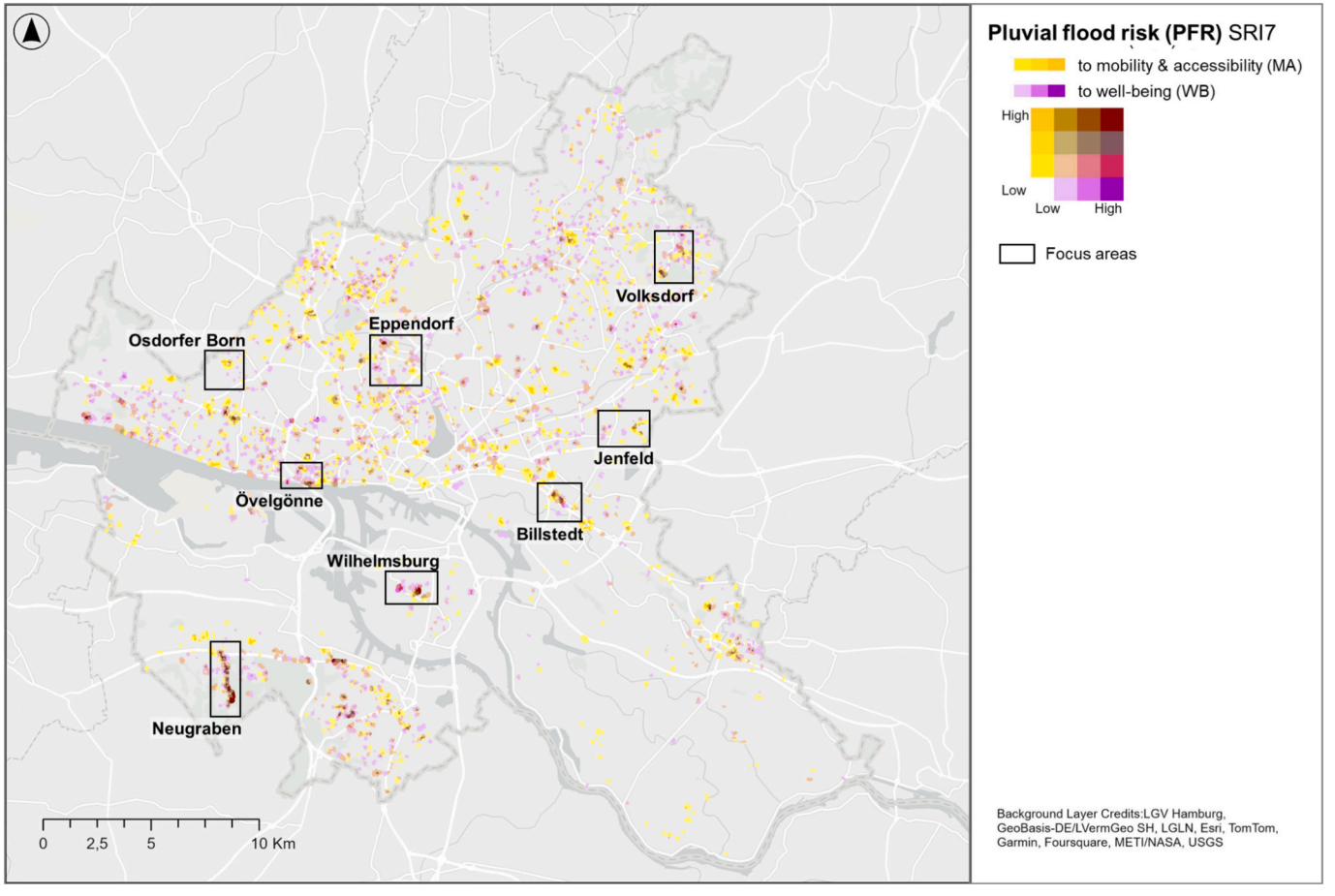


Fig. 4. Pluvial flood risks for Hamburg (PFR_{MA} & PFR_{WB}). The map presents the spatial distribution of pluvial flood risk (PFR) in Hamburg, differentiating between risks to mobility and accessibility (PFR_{MA}, yellow) and risks to well-being (PFR_{WB}, purple). The color gradient represents the intensity of overlapping risks, with darker shades indicating areas of higher combined risk. The map highlights focus areas (black rectangles) where both risk types co-occur, identifying potential hotspots of pluvial flood vulnerability. The background layer provides geographic context, including road networks and waterways. (For interpretation of the references to color in this figure legend, the reader is referred to the web version of this article.)

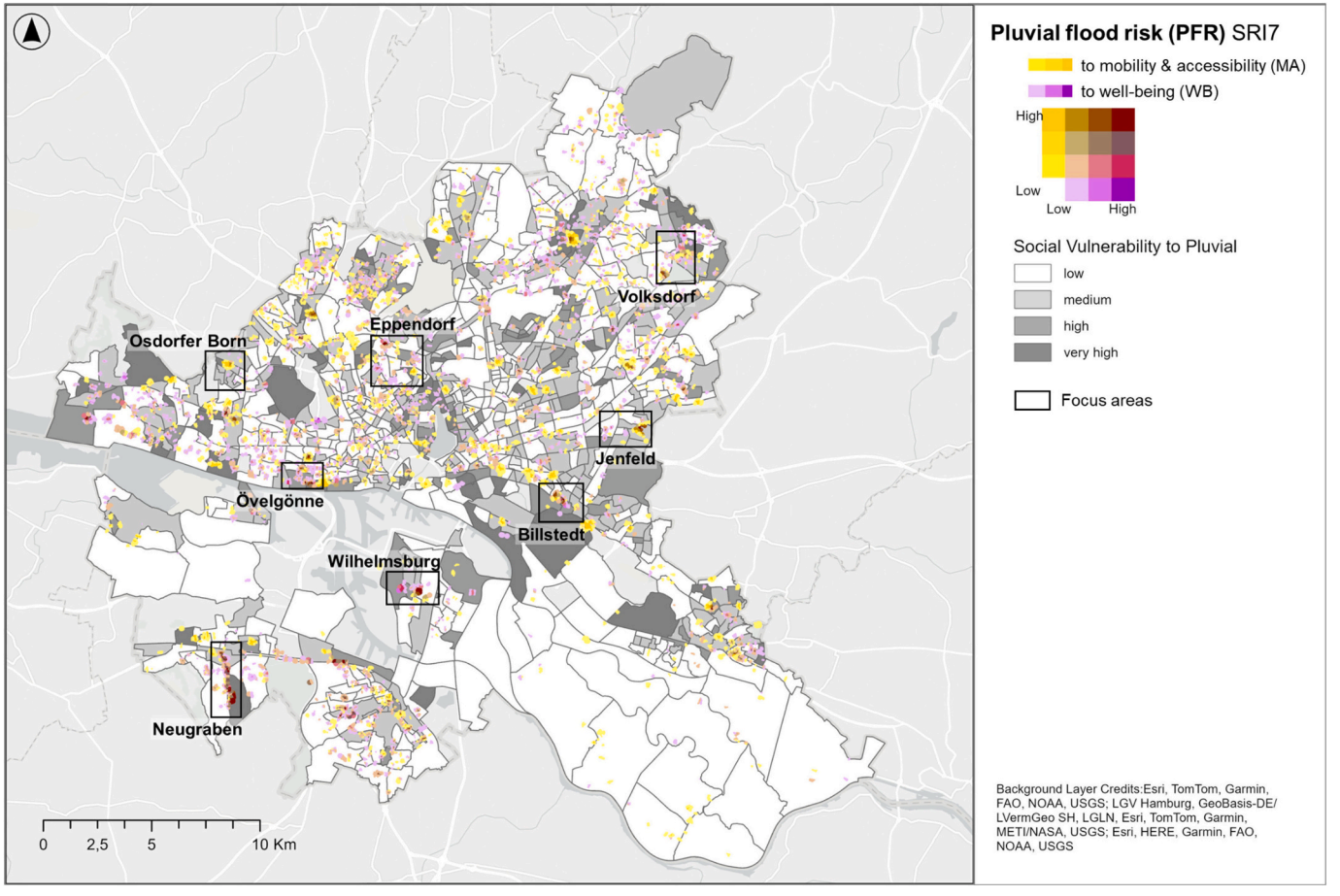


Fig. 5. Combined presentation of social vulnerability and pluvial flood risks for Hamburg. This map illustrates the relationship between pluvial flood risk (PFR) and social vulnerability in Hamburg. Grey areas represent neighborhoods with medium to very high socio-economic sensitivity to climate-related hazards. The colored gradients indicate PFRs to mobility and accessibility (yellow) and well-being (purple). The overlay of these two datasets identifies areas where socially vulnerable populations are disproportionately affected by pluvial flooding. Black squares highlight focus areas within Hamburg. (For interpretation of the references to color in this figure legend, the reader is referred to the web version of this article.)

such as Billstedt and Osdorfer Born, where high sensitivity and low coping capacity amplify the overall risk (Fig. 6). Billstedt exhibits a risk pattern, with elevated levels of social vulnerability contributing to heightened PFRs. This may affect their ability to reach workplaces, medical facilities, and emergency services during extreme weather events. The socio-economic structure of the district, characterized by a large proportion of lower-income households and residents with limited coping capacity, increases the adverse effects of pluvial floods. Addressing both physical exposure and socio-economic vulnerabilities is crucial to enhancing resilience in this area.

Osdorfer Born presents a case where mobility-related risks are particularly prominent. The district is home to a high concentration of socioeconomically vulnerable residents, many of whom rely heavily on public transportation. During pluvial flood events, critical roads and pathways become impassable, disrupting daily commutes and emergency responses. While the direct impact on residential buildings is comparatively lower, the overall well-being of residents may still be significantly affected due to restricted access to essential services. This case highlights the necessity of improving flood-adaptive infrastructure and public transit resilience in areas where mobility disruptions dominate.

Areas such as Ovelgönne and Eppendorf suffer from high sensitivity of the residents as the main driver of SV_{PF}. In Övelgönne the dominance of PFR_{WB} is clearly visible. Due to the location on the *Geest* slope, the sides of the buildings facing the slope show increased water levels, as the houses dam up the water flowing over the surface of the slope. However, unlike in other high-risk areas, the road networks are not flooded, which is why the according PFR_{MA} values are low.

Despite its relatively dense urban structure, Eppendorf exhibits lower mobility-related flood risks while still displaying significant well-being-related risks. The increased risk to well-being is likely due to ground-floor housing that is more susceptible to water ingress. However, flood-resilient road infrastructure and well-connected road networks mitigate the risk of accessibility disruptions, highlighting the importance of differentiating between risk dimensions when designing intervention strategies.

In turn, in areas like Wilhelmsburg and Jenfeld, the residents show low coping capacity as the main contributing factor to SV_{PF}. Jenfeld thereby serves as a key example of an area where mobility risks exist in isolation from well-being risks, because residential buildings remain largely unaffected by direct water ingress. This pattern underscores the importance of considering indirect flood impacts, such as accessibility barriers, when developing comprehensive flood risk assessments.

At the same time, our assessment also identifies urban areas with good coping capacity, but which are particularly affected by a high potential impact of the pluvial flooding hazard indices (Volksdorf).

5.3. Limitations

While this study provides a comprehensive assessment of pluvial flood risk in Hamburg, several limitations must be considered:
Conceptual limitations

- While our risk implementation is based on the IPCC model of 2022, human responses to risk are not explicitly represented in our framework. Technical adaptation measures (e.g. the sewer system) are already embedded in the hazard modeling. Future versions of the presented framework could include responses for all presented risk parameters, for example through agent-based modeling (Peng et al., 2023; Yang et al., 2018a).
- While drainage capacity, infiltration rates, and retention measures are indirectly considered in hazard modeling, explicit inclusion of emergency response measures and long-term adaptation strategies would enhance the model's applicability for decision-makers.
- Our current assessment does not incorporate the dynamic character of risk (in the sense that risk in reality depends on constantly changing sub-indices) (Skougaard Kaspersen et al., 2017; Stolte et al., 2024; Swain et al., 2020), as we base our risk calculation on stationary data. However, our framework is able to include dynamic hazard, exposure, and vulnerability given that according data or projections are available.

Social vulnerability assessment

- The assessment of social vulnerability relies on selected demographic variables, the weighting scheme used in the TOPSIS method, and the assumption that social vulnerability remains constant within statistical units. This overlooks local variations in vulnerability that typically exist within neighborhoods (i.e. not 0.3 children live in each house, but 0 in some houses and 1 or 2 children in others).
- The simple disaggregation of social data to buildings generally introduces systematic bias, when building-specific data is not available. For smaller study areas or even more aggregated social data, different or additional assumptions should be made to reduce the error.
- The assumption that mixed-use buildings lack residents on the ground floor and that population density is uniform within statistical units may lead to additional inaccuracies. Furthermore, rents for ground-floor flats are typically lower in some neighborhoods, which could be associated with lower coping capacity of ground-floor residents in general. Residents who are dependent on barrier-free apartments on the first floor (no stairs) also typically have a higher sensitivity (age; physical challenges), not accounted for.

Methodological assumptions

- Several methodological choices rely heavily on expert judgement, including the selection of hazard thresholds, buffer distances, indicator weights, and index transformations. Thus, we acknowledge different outcomes if other buffer sizes are used. Our

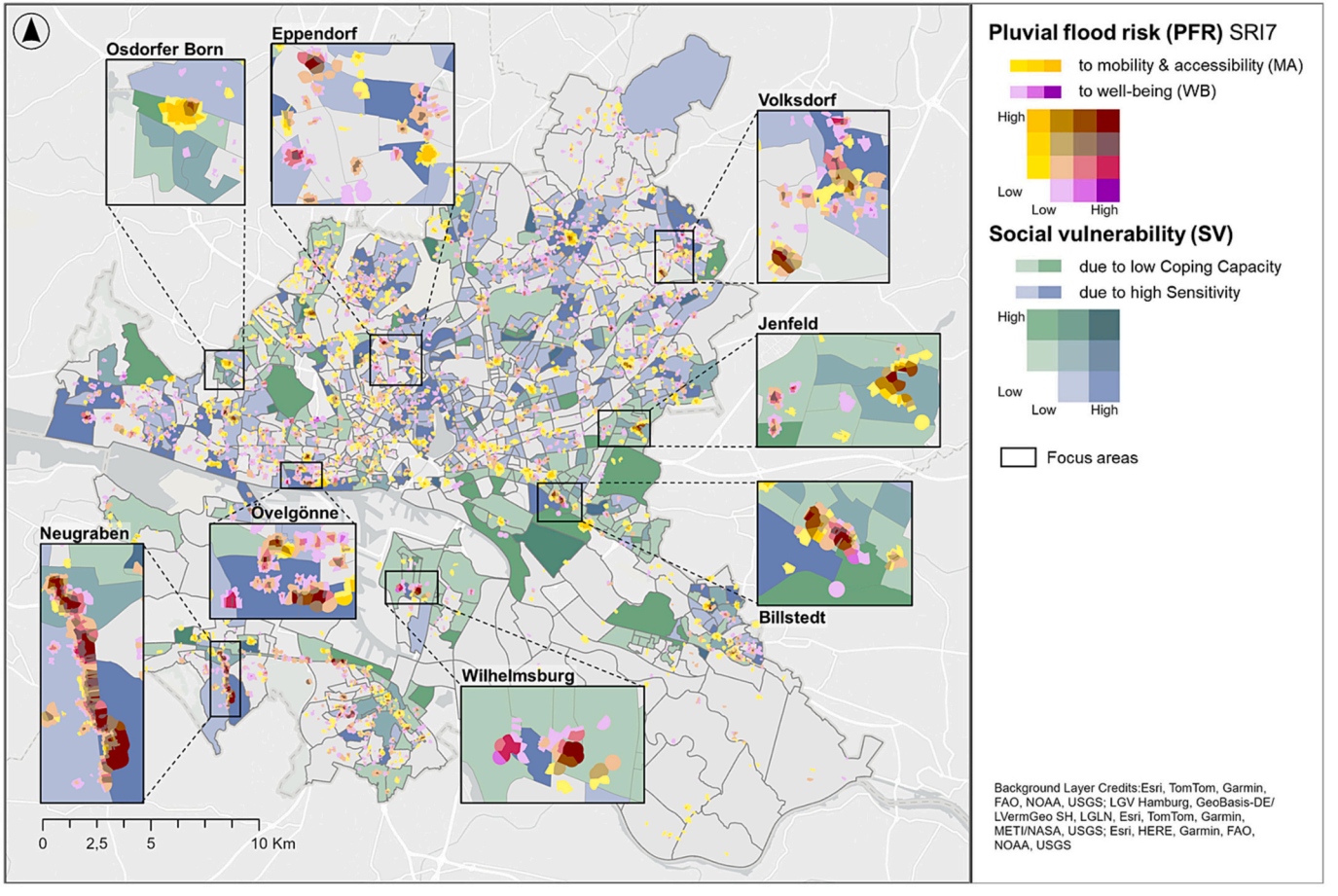


Fig. 6. Combined depiction of social vulnerability indicators (coping capacity and sensitivity) and pluvial flood risk for Hamburg. Darker green color shades represent high social vulnerability due to low coping capacity while darker blue color shades indicate high social vulnerability due to high sensitivity. Dark green-blueish represents compound areas of high social vulnerability related to low coping capacity and high sensitivity. The yellow and purple color gradients indicate PFRs to mobility and accessibility (yellow) and well-being (purple). Black squares highlight focus areas within Hamburg. Blow-ups show a 3.5× magnified view of the focus areas. (For interpretation of the references to color in this figure legend, the reader is referred to the web version of this article.)

assessment of PFR_{WB} is based on flood thresholds starting at 30 cm, whereby individual houses or even entire neighborhoods have raised ground floors (“*Hochparterre*”) (Brandenburger and Kähler, 1988). Future inclusion of flow velocity could enhance the approximation of risks (well-being as well as mobility).

- The proposed risk indices do not represent all possible consequences of pluvial flooding, such as failures of critical building utilities. Additional exposure definitions may be required depending on the intended application.
- On the one hand, the usage of Delaunay-Triangulation method and smoothing functions aids in presenting the results in a structured manner while maintaining hotspot areas. On the other hand, the methods applied obscure small-scale variations in risk, especially if smoothing is applied several times. The iterative application of this method allows a good amount of control over the smoothing effect.

Validation and uncertainty

- This framework is at its current state only verified by experts. Emergency calls, insurance losses or citizen reports would be valuable data sources to further verify the results presented. These might be used to adjust the thresholds and weights within the framework. We further acknowledge the lack of historical high-resolution inundation reports as limitation, which could help in validating the results.
- This study does not feature a formal uncertainty assessment. We argue that uncertainty depends on uncertainties arising from the input data, the selected indicators, and the applied thresholds and methodological assumptions.. Vogelbacher et al. (2026) applied a sensitivity analysis to better understand the effects of the applied thresholds. Future work should include sensitivity and uncertainty analyses to quantify their influence on the resulting risk patterns.

Transfeability

- The framework has potential for transferability, however, its application in other urban contexts depends on the availability of high-resolution hazard, exposure, and socio-economic data. Furthermore, city-specific conditions, including urban morphology, demographic structures, and flood characteristics, require local adaptation of the framework.

6. Conclusion and outlook

General insights

- Social vulnerability is spatially decoupled from hazard: areas with high flood hazard are not necessarily the same areas with high social vulnerability. This implies that pluvial flood risk cannot be inferred from hazard maps alone.
- Exposure should be differentiated and relational, not just spatial. Rather than treating exposure as simple population presence, the study links specific population groups to specific facets of the hazard.
- High-resolution data fundamentally changes risk insights. Using building-level and fine-scale data reveals micro-scale hotspots, and intra-neighborhood inequalities. Risk is highly scale-dependent, coarse data can obscure critical local risk patterns.

This analysis accounts for the multidimensionality of urban flood risk. By highlighting the complex interplay between socio-economic vulnerability, exposure and hazard, it emphasizes the need for a holistic risk assessment. While physical exposure to flooding is a key determinant of risk, the inclusion of social vulnerability (SV_{PF}) allows for a deeper understanding of how social and demographic factors compound this risk. This integrated approach may help to target interventions in high-risk areas according to the risk drivers, such as flood resilient infrastructure, community preparedness programs, and improve social services for vulnerable populations.

The methodological approach employed, particularly the use of TOPSIS, Shannon entropy, and the multiple methodological decisions regarding the modeling of exposure and hazard, supports a systematic assessment of risk which can be further validated through additional stakeholder input. The spatial smoothing process applied to the risk values allows the identification of critical hotspots while preserving detail, without compromising privacy issues. The Voronoi cells enable the integration of individual building-level risks into a broader spatial context. Most importantly, by distinguishing between well-being and mobility risk at high spatial resolution, the framework supports targeted urban flood risk management and urban adaptation planning by identifying both high-risk areas and their underlying risk drivers.

The results also indicate the potential for transferability of this framework. By incorporating both small-scale local conditions and socio-economic patterns at city level, the methodology can serve as a basis for risk management strategies in other urban areas. In this context, local knowledge and stakeholders are essential for adapting the framework to the specific characteristics of each city. Future studies should investigate the integration of temporal dynamics, such as changes in climate patterns or urban development, to further refine these risk assessments. Moreover, additional research is needed to explore how human responses and adaptive capacities influence pluvial flood risks. Integrating real-time data could enhance predictive accuracy and decision-making processes.

These findings underscore the need for integrative adaptation planning that considers both social and infrastructural resilience when addressing urban flood risk. Making transparent where and how vulnerability is reproduced as part of risk assessments can profoundly enhance practitioners' understanding of risk and thus inform more in-depth policy instruments (Teebken, 2024). This study contributes to informed policy decisions that allocate resources efficiently to protect the most vulnerable populations and enhance

urban resilience to future flood events. In this context, community engagement and participatory approaches have been shown to be valuable methods which should be included and prioritized in flood risk management and climate change adaptation planning (Ross et al., 2015; Wamsler, 2017).

Transdisciplinary collaboration between urban planners, public health experts, and climate scientists is crucial to develop urban climate adaptation and flood risk management policies that align with both immediate needs and long-term resilience goals. Recent studies highlight the role of land-use characteristics, blue-green infrastructure, and nature-based solutions in enhancing flood regulation ecosystem services and urban resilience (Veerkamp et al., 2021; Huang et al., 2020; Hanf et al., 2025; Shi et al., 2026). Linking high-resolution social flood risk assessments with ecosystem services could therefore support more effective flood risk governance.

In summary, the results provide valuable insights into the distribution of health-related risks from pluvial floods in Hamburg. This study is particularly effective in analyzing the root causes, in order to understand how various contextual conditions contribute to the overall urban pluvial flood risk. By identifying both small-scale hotspots and larger at-risk areas, this study offers a solid foundation for justice-oriented climate policy approaches and action, making vulnerable populations a front and center concern (Diezmartínez and Short Gianotti, 2022; Strange et al., 2024) and thus facilitating targeted interventions and guiding future planning efforts to enhance flood resilience in the city.

Despite these strengths, several limitations should be acknowledged. The social vulnerability assessment is constrained by the small number of indicators and does not capture all dimensions of vulnerability. Likewise, the applied hazard thresholds are based on current literature and methodological assumptions, and alternative threshold definitions will influence the resulting risk patterns. Finally, the proposed framework has not yet been empirically validated against observed flood impacts or health outcomes. Future research should therefore address empirical validation, i.e. through post-event observations, insurance or damage records or emergency response data, to further assess the robustness and applicability of the framework.

Supplementary data to this article can be found online at https://doi.org/10.1016/j.crm.2026.100893.

Data statement

The hazard data used is publicly available. The social data can be requested from the authors.

CRediT authorship contribution statement

Malte von Szombathely: Writing – review & editing, Writing – original draft, Visualization, Validation, Supervision, Project administration, Methodology, Investigation, Formal analysis, Data curation, Conceptualization. **Jörn Behrens:** Writing – review & editing. **Franziska Stefanie Hanf:** Writing – review & editing, Conceptualization. **Marc Lennartz:** Writing – review & editing, Writing – original draft, Visualization, Validation, Methodology, Investigation, Formal analysis, Data curation, Conceptualization. **Shefali Nayak:** Writing – review & editing. **Jürgen Oßenbrügge:** Writing – review & editing, Funding acquisition, Conceptualization. **Benjamin Poschlod:** Writing – review & editing, Writing – original draft, Visualization, Validation, Supervision, Methodology, Investigation, Formal analysis, Data curation, Conceptualization. **Jürgen Scheffran:** Writing – review & editing. **Anastasia Vogelbacher:** Writing – review & editing, Writing – original draft, Visualization, Validation, Methodology, Investigation, Formal analysis, Data curation, Conceptualization. **Jana Sillmann:** Writing – review & editing, Funding acquisition, Conceptualization.

Declaration of competing interest

The authors declare that they have no known competing financial interests or personal relationships that could have appeared to influence the work reported in this paper.

Acknowledgements

This work was funded by the Deutsche Forschungsgemeinschaft (DFG, German Research Foundation) under Germany's Excellence Strategy — EXC 2037 “CLICCS – Climate, Climatic Change, and Society” — Project No. 390683824, contribution to the Center for Earth System Research and Sustainability (CEN) of Universität Hamburg. Advice for fair data guidelines provided by the FAIR2Adapt project (Horizon Europe Framework Programme, grant agreement No. 101188256) are greatly acknowledged. We thank Hamburg's “Behörde für Umwelt, Klima, Energie und Agrarwirtschaft (BUKEA)” for providing data on flooding risks and heavy rains and the “Statistisches Amt für Hamburg und Schleswig-Holstein (Statistikamt Nord)” for providing administrative and social data. We also acknowledge the Landesbetrieb für Geoinformation und Vermessung for making most of the data used in this study freely available at the Geoportal Hamburg (https://geoportal-hamburg.de). We acknowledge financial support from the Open Access Publication Fund of Universität Hamburg.

Appendix A. Supplementary data

Supplementary data to this article can be found online at https://doi.org/10.1016/j.crm.2026.100893.

Data availability

Data will be made available on request.

References

Abebe, Y.A., Ghorbani, A., Nikolic, I., Manojlovic, N., Gruhn, A., Vojinovic, Z., 2020. The role of household adaptation measures in reducing vulnerability to flooding: a coupled agent-based and flood modelling approach. Hydrol. Earth Syst. Sci. 24, 5329–5354. https://doi.org/10.5194/hess-24-5329-2020.

Allegri, E., Zanetti, M., Torresan, S., Critto, A., 2024. Pluvial flood risk assessment for 2021–2050 under climate change scenarios in the Metropolitan City of Venice. Sci. Total Environ. 914, 169925. https://doi.org/10.1016/j.scitotenv.2024.169925.

Bhola, P.K., Leandro, J., Disse, M., 2020. Building hazard maps with differentiated risk perception for flood impact assessment. Nat. Hazards Earth Syst. Sci. 20, 2647–2663. https://doi.org/10.5194/nhess-20-2647-2020.

Bignami, D.F., 2019. Flood Proofing in Urban Areas. Springer International Publishing AG, Cham.

Bischoff, G., Wahl, J., Döring, J., 2021. Entwässerungsanalyse für Starkregen – Neugraben-Fischbek.

Blöschl, G., Buttinger-Kreuzhuber, A., Cornel, D., Eisl, J., Hofer, M., Hollaus, M., Horváth, Z., Komma, J., Konev, A., Parajka, J., Pfeifer, N., Reithofer, A., Salinas, J., Valent, P., Výleta, R., Waser, J., Wimmer, M.H., Stiefelmeyer, H., 2024. Hyper-resolution flood hazard mapping at the national scale. Nat. Hazards Earth Syst. Sci. 24, 2071–2091. https://doi.org/10.5194/nhess-24-2071-2024.

Boultif, M., Hafnaoui, M.A., 2026. Prioritizing flood vulnerability hotspots: an integrated AHP and TOPSIS framework, case study of El Bayadh city, western Algeria. J. Afr. Earth Sci. 240, 106166. https://doi.org/10.1016/j.jafrearsci.2026.106166.

Brandenburger, D., Kähler, G., 1988. Das Etagenhaus um 1900: “Schlitzbauten” um 1910 Isestraße. In: Brandenburger, D., Kähler, G. (Eds.), Architektour. Vieweg+Teubner Verlag, Wiesbaden, pp. 214–217. https://doi.org/10.1007/978-3-322-85411-7_53.

Buttinger-Kreuzhuber, A., Horváth, Z., Noelle, S., Blöschl, G., Waser, J., 2019. A fast second-order shallow water scheme on two-dimensional structured grids over abrupt topography. Adv. Water Resour. 127, 89–108. https://doi.org/10.1016/j.advwatres.2019.03.010.

Buttinger-Kreuzhuber, A., Konev, A., Horváth, Z., Cornel, D., Schwerdorf, I., Blöschl, G., Waser, J., 2022a. An integrated GPU-accelerated modeling framework for high-resolution simulations of rural and urban flash floods. Environ. Model. Softw. 156, 105480. https://doi.org/10.1016/j.envsoft.2022.105480.

Buttinger-Kreuzhuber, A., Waser, J., Cornel, D., Horváth, Z., Konev, A., Wimmer, M.H., Komma, J., Blöschl, G., 2022b. Locally relevant high-resolution hydrodynamic Modeling of river floods at the regional scale. Water Resour. Res. 58, e2021WR030820. https://doi.org/10.1029/2021WR030820.

Calianno, M., Ruin, I., Gourley, J.J., 2013. Supplementing flash flood reports with impact classifications. J. Hydrol. 477, 1–16. https://doi.org/10.1016/j.jhydrol.2012.09.036.

Chan, S.C., Kendon, E.J., Roberts, N.M., Fowler, H.J., Blenkinsop, S., 2016. The characteristics of summer sub-hourly rainfall over the southern UK in a high-resolution convective permitting model. Environ. Res. Lett. 11, 094024. https://doi.org/10.1088/1748-9326/11/9/094024.

Cutter, S.L., Boruff, B.J., Shirley, W.L., 2003. Social vulnerability to environmental hazards. Soc. Sci. Q. 84, 242–261. https://doi.org/10.1111/1540-6237.8402002.

De Guttry, C., Ratter, B., 2022. Expiry date of a disaster: memory anchoring and the storm surge 1962 in Hamburg, Germany. Int. J. Disaster Risk Reduct. 70, 102719. https://doi.org/10.1016/j.ijdrr.2021.102719.

Delaunay, B., 1934. Sur la sphère vide. A la mémoire de Georges Voronoi. Bull. L’Académie Sci. L’URSS Cl. Sci. Mathématiques Na 793–800.

Deutscher Wetterdienst (DWD) (Ed.): Klimareport Hamburg, Behörde für Umwelt, Klima, Energie und Agrarwirtschaft, Offenbach am Main, Deutschland, 56 pp., ISBN 978-3-88148-530-2, 2021.

Dewan, A., 2013. Flood in a megacity: geospatial techniques in assessing hazards, Risk and Vulnerability, Floods in a Megacity: Geospatial Techniques in Assessing Hazards, Risk and Vulnerability. https://doi.org/10.1007/978-94-007-5875-9.

Diezmartínez, C.V., Short Gianotti, A.G., 2022. US cities increasingly integrate justice into climate planning and create policy tools for climate justice. Nat. Commun. 13, 5763. https://doi.org/10.1038/s41467-022-33392-9.

Durst, D., Lämmel, G., Klüpfel, H., 2014. Large-scale multi-modal evacuation analysis with an application to Hamburg. In: Weidmann, U., Kirsch, U., Schreckenberg, M. (Eds.), Pedestrian and Evacuation Dynamics 2012. Springer International Publishing, Cham, pp. 361–369. https://doi.org/10.1007/978-3-319-02447-9_30.

Ekmekcioğlu, Ö., Koc, K., Özger, M., 2021. Stakeholder perceptions in flood risk assessment: a hybrid fuzzy AHP-TOPSIS approach for Istanbul, Turkey. Int. J. Disaster Risk Reduct. 60, 102327. https://doi.org/10.1016/j.ijdrr.2021.102327.

Falconer, R.H., Cobby, D., Smyth, P., Astle, G., Dent, J., Golding, B., 2009. Pluvial flooding: new approaches in flood warning, mapping and risk management. J. Flood Risk Manag. 2, 198–208. https://doi.org/10.1111/j.1753-318X.2009.01034.x.

Fariza, A., Hasim, J.A.N., Rahadianto, H., 2015. Flood risk mapping of Bengawan solo river in east java using the analytic hierarchy process and head/tails break classification. . Presented at the 2015 International Conference on Science in Information Technology (ICSITech),. IEEE, Yogyakarta, pp. 331–336. https://doi.org/10.1109/ICSITech.2015.7407827.

Fekete, A., Rufat, S., 2023. Should everyone in need be treated equally? A European survey of expert judgment on social vulnerability to floods and pandemics to validate multi-hazard vulnerability factors. Int. J. Disaster Risk Reduct. 85, 103527. https://doi.org/10.1016/j.ijdrr.2023.103527.

Fereshtehpour, M., Najafi, M.R., 2025. Urban stormwater resilience: global insights and strategies for climate adaptation. Urban Clim. 59, 102290. https://doi.org/10.1016/j.uclim.2025.102290.

FHH, Behörde für Umwelt, Klima, Energie und Agrarwirtschaft, 2024. Technisches Informationsblatt Starkregengefahrenkarte Hamburg. https://www.hamburg.de/resource/blob/173730/5270f2cb96a1e41b5e45b64f84aa853e/d-technischesinformationsblatt-srgk-data.pdf.

FHH, Landesbetrieb Geoinformation und Vermessung, 2017. INSPIRE HH Verkehrsnetze ALKIS (Version 3.2) [Data set]. https://metaver.de/trefferanzeige?cmd=doShowDocument&docuuid=1BD1BACC-6E6C-40E2-9B29-3B851CD6CFB5.

FHH, Landesbetrieb Geoinformation und Vermessung, 2020. INSPIRE HH Gebäude ALKIS (Version 3.2) [Data set]. https://metaver.de/trefferanzeige?docuuid=0C4AD3A9-ECC4-4936-92FD-18E21DFA9234.

FHH, Statistikamt Nord, 2017. Statistische Gebiete in Hamburg (Version 2016) [Data set]. https://metaver.de/trefferanzeige?docuuid=DB93B23B-D3F1-4460-8C62-DD1961893767&q=statistische%20gebiete%20hamburg%20.

FHH, Statistikamt Nord, 2024. Bevölkerung in Hamburg am 31.12.2023 [Data set]. https://www.statistik-nord.de/zahlen-fakten/hamburger-melderegister/bevoelkerungsstand#c6618.

Field, C.B., Barros, V.R., Intergovernmental Panel on Climate Change, 2014. Climate Change 2014: Impacts, Adaptation, and Vulnerability: Working Group II Contribution to the Fifth Assessment Report of the Intergovernmental Panel on Climate Change. Cambridge University Press, New York, NY.

Fosser, G., Kendon, E.J., Stephenson, D., Tucker, S., 2020. Convection-permitting models offer promise of more certain extreme rainfall projections. Geophys. Res. Lett. 47, e2020GL088151. https://doi.org/10.1029/2020GL088151.

Fosser, G., Gaetani, M., Kendon, E.J., Adinolfi, M., Ban, N., Belušić, D., Caillaud, C., Careto, J.A.M., Coppola, E., Demory, M.-E., De Vries, H., Dobler, A., Feldmann, H., Goergen, K., Lenderink, G., Pichelli, E., Schär, C., Soares, P.M.M., Somot, S., Tölle, M.H., 2024. Convection-permitting climate models offer more certain extreme rainfall projections. Npj Clim. Atmos. Sci. 7, 51. https://doi.org/10.1038/s41612-024-00600-w.

Fowler, H.J., Lenderink, G., Prein, A.F., Westra, S., Allan, R.P., Ban, N., Barbero, R., Berg, P., Blenkinsop, S., Do, H.X., Guerreiro, S., Haerter, J.O., Kendon, E.J., Lewis, E., Schaer, C., Sharma, A., Villarini, G., Wasko, C., Zhang, X., 2021. Anthropogenic intensification of short-duration rainfall extremes. Nat. Rev. Earth Environ. 2, 107–122. https://doi.org/10.1038/s43017-020-00128-6.

Fox, S., Agyemang, F., Hawker, L., Neal, J., 2024. Integrating social vulnerability into high-resolution global flood risk mapping. Nat. Commun. 15, 3155. https://doi.org/10.1038/s41467-024-47394-2.

Fritsch, K., Assmann, A., Tyrna, B., 2016. Long-term experiences with pluvial flood risk management. E3S Web Conf. 7, 04017. https://doi.org/10.1051/e3sconf/20160704017.
Fuchs, S., Karagiorgos, K., Keiler, M., Papathoma-Köhle, M., Nyberg, L., 2024. The ambiguity in IPCC'S risk diagram raises explanatory challenges. Nat. Hazards 120, 12559–12564. https://doi.org/10.1007/s11069-024-06643-9.
Guan, X., Vorogushyn, S., Apel, H., Merz, B., 2023. Assessing compound pluvial-fluvial flooding: research status and ways forward. Water Secur. 19, 100136. https://doi.org/10.1016/j.wasec.2023.100136.
Guerreiro, S.B., Fowler, H.J., Barbero, R., Westra, S., Lenderink, G., Blenkinsop, S., Lewis, E., Li, X.-F., 2018. Detection of continental-scale intensification of hourly rainfall extremes. Nat. Clim. Chang. 8, 803–807. https://doi.org/10.1038/s41558-018-0245-3.
Hammond, M.J., Chen, A.S., Djordjević, S., Butler, D., Mark, O., 2015. Urban flood impact assessment: a state-of-the-art review. Urban Water J. 12, 14–29. https://doi.org/10.1080/1573062X.2013.857421.
Hanf, F.S., Meier, L., Hawxwell, T., Oßenbrügge, J., Knieling, J., Sillmann, J., 2024. "Narrative images" as a learning approach: (transformative) adaptation scenarios for dealing with urban water risks in Hamburg, Germany. Front. Sustain. Cities 6, 1430257. https://doi.org/10.3389/frsc.2024.1430257.
Hanf, F.S., Ament, F., Boettcher, M., Burgemeister, F., Gaslikova, L., Hoffmann, P., Knieling, J., Matthias, V., Meier, L., Pein, J., Poschlod, B., Quante, M., Ratzke, L., Rudolph, E., Scheffran, J., Schlünzen, K.H., Shokri, N., Sillmann, J., Vogelbacher, A., von Szombathely, M., Wickel, M., 2025. Towards a socio-ecological system understanding of urban flood risk and barriers to climate change adaptation using causal loop diagrams. Int. J. Urban Sustain. Dev. https://doi.org/10.1080/19463138.2025.2474399.
Haslinger, K., Breinl, K., Pavlin, L., Pistotnik, G., Bertola, M., Olefs, M., Greilinger, M., Schöner, W., Blöschl, G., 2025. Increasing hourly heavy rainfall in Austria reflected in flood changes. Nature 639, 667–672. https://doi.org/10.1038/s41586-025-08647-2.
He, H., Li, R., Pei, J., Bilodeau, J.-P., Huang, G., 2023. Current overview of impact analysis and risk assessment of urban pluvial flood on road traffic. Sustain. Cities Soc. 99, 104993. https://doi.org/10.1016/j.scs.2023.104993.
Huang, Y., Tian, Z., Ke, Q., et al., 2020. Nature-based solutions for urban pluvial flood risk management. WIREs Water. 7, e1421. https://doi.org/10.1002/wat2.1421.
Hwang, C.-L., Yoon, K., 1981. Multiple Attribute Decision Making, Lecture Notes in Economics and Mathematical Systems. Springer, Berlin, Heidelberg. https://doi.org/10.1007/978-3-642-48318-9.
Ji, J., Wang, D., 2023. Evaluation analysis and strategy selection in urban flood resilience based on EWM-TOPSIS method and graph model. J. Clean. Prod. 425, 138955. https://doi.org/10.1016/j.jclepro.2023.138955.
Jiang, B., 2013. Head/tail breaks: a new classification scheme for data with a heavy-tailed distribution. Prof. Geogr. 65, 482–494. https://doi.org/10.1080/00330124.2012.700499.
Jiang, S., Tarasova, L., Yu, G., Zscheischler, J., 2024. Compounding effects in flood drivers challenge estimates of extreme river floods. Sci. Adv. 10, eadl4005. https://doi.org/10.1126/sciadv.adl4005.
Judt, F., 2018. Insights into atmospheric predictability through global convection-permitting model simulations. J. Atmos. Sci. 75, 1477–1497. https://doi.org/10.1175/JAS-D-17-0343.1.
Kendon, E.J., Blenkinsop, S., Fowler, H.J., 2018. When will we detect changes in Short-duration precipitation extremes? J. Clim. 31, 2945–2964. https://doi.org/10.1175/JCLI-D-17-0435.1.
Kendon, E.J., Fischer, E.M., Short, C.J., 2023. Variability conceals emerging trend in 100yr projections of UK local hourly rainfall extremes. Nat. Commun. 14, 1133. https://doi.org/10.1038/s41467-023-36499-9.
Kron, W., 2005. Flood Risk = Hazard • Values • Vulnerability. Water Int. 30, 58–68. https://doi.org/10.1080/02508060508691837.
Lamond, J.E., Joseph, R.D., Proverbs, D.G., 2015. An exploration of factors affecting the long term psychological impact and deterioration of mental health in flooded households. Environ. Res. 140, 325–334. https://doi.org/10.1016/j.envres.2015.04.008.
Lang, A., Poschlod, B., 2024. Updating catastrophe models to today's climate – an application of a large ensemble approach to extreme rainfall. Clim. Risk Manag. 44, 100594. https://doi.org/10.1016/j.crm.2024.100594.
Lavin-Gullon, A., Fernandez, J., Bastin, S., Cardoso, R.M., Fita, L., Giannaros, T.M., Goergen, K., Gutierrez, J.M., Kartsios, S., Katragkou, E., Lorenz, T., Milovac, J., Soares, P.M.M., Sobolowski, S., Warrach-Sagi, K., 2021. Internal variability versus multi-physics uncertainty in a regional climate model. Int. J. Climatol. 41. https://doi.org/10.1002/joc.6717.
Lazzarin, T., Viero, D.P., Molinari, D., Ballio, F., Defina, A., 2022. Flood damage functions based on a single physics- and data-based impact parameter that jointly accounts for water depth and velocity. J. Hydrol. 607, 127485. https://doi.org/10.1016/j.jhydrol.2022.127485.
Lind, P., Belušić, D., Médus, E., Dobler, A., Pedersen, R.A., Wang, F., Matte, D., Kjellström, E., Landgren, O., Lindstedt, D., Christensen, O.B., Christensen, J.H., 2023. Climate change information over Fenno-Scandinavia produced with a convection-permitting climate model. Clim. Dyn. 61, 519–541. https://doi.org/10.1007/s00382-022-06589-3.
Lockwood, J.W., Lin, N., Gori, A., Oppenheimer, M., 2024. Increasing flood hazard posed by tropical cyclone rapid intensification in a changing climate. Geophys. Res. Lett. 51, e2023GL105624. https://doi.org/10.1029/2023GL105624.
Maaß, F., Huang, Z., 2024. Sozialmonitoring Integrierte Stadtteilentwicklung – Bericht 2024. FHH, BSW, Hamburg.
Maaß, F., Vorkoeper, J., Kaiser, A., 2023. Sozialmonitoring Integrierte Stadtteilentwicklung – Karten- und Tabellenband 2023. FHH, BSW, Hambug.
Marbaix, P., Magnan, A.K., Muccione, V., Thorne, P.W., Zommers, Z., 2025. Climate change risks illustrated by the Intergovernmental Panel on Climate Change (IPCC) "burning embers.". Earth Syst. Sci. Data 17, 317–349. https://doi.org/10.5194/essd-17-317-2025.
Marra, F., Koukoula, M., Canale, A., Peleg, N., 2024. Predicting extreme sub-hourly precipitation intensification based on temperature shifts. Hydrol. Earth Syst. Sci. 28, 375–389. https://doi.org/10.5194/hess-28-375-2024.
Nguyen, H.X., Nguyen, An Thinh, Ngo, A.T., Phan, V.T., Nguyen, T.D., Do, V.T., Dao, D.C., Dang, D.T., Nguyen, Anh Tuan, Nguyen, T.K., Hens, L., 2020. A hybrid approach using GIS-based fuzzy AHP–TOPSIS assessing flood hazards along the south-central coast of Vietnam. Appl. Sci. 10, 7142. https://doi.org/10.3390/app10207142.
Pathan, A.I., Girish Agnihotri, P., Said, S., Patel, D., 2022. AHP and TOPSIS based flood risk assessment- a case study of the Navsari City, Gujarat, India. Environ. Monit. Assess. 194, 509. https://doi.org/10.1007/s10661-022-10111-x.
Peng, Y., Rodriguez Lopez, J.M., Santos, A.P., Mobeen, M., Scheffran, J., 2023. Simulating exposure-related human mobility behavior at the neighborhood-level under COVID-19 in Porto Alegre, Brazil. Cities 134, 104161. https://doi.org/10.1016/j.cities.2022.104161.
Poschlod, B., 2022. Attributing heavy rainfall event in Berchtesgadener land to recent climate change – further rainfall intensification projected for the future. Weather Clim. Extrem. 38, 100492. https://doi.org/10.1016/j.wace.2022.100492.
Poschlod, B., Koh, J., 2024. Convection-permitting climate models can support observations to generate rainfall return levels. Water Resour. Res. 60, e2023WR035159. https://doi.org/10.1029/2023WR035159.
Poschlod, B., Ludwig, R., 2021. Internal variability and temperature scaling of future sub-daily rainfall return levels over Europe. Environ. Res. Lett. 16, 064097. https://doi.org/10.1088/1748-9326/ac0849.
Poschlod, B., Hodnebrog, Ø., Wood, R.R., Alterskjær, K., Ludwig, R., Myhre, G., Sillmann, J., 2018. Comparison and evaluation of statistical rainfall disaggregation and high-resolution dynamical downscaling over complex terrain. J. Hydrometeorol. 19, 1973–1982. https://doi.org/10.1175/JHM-D-18-0132.1.
Poschlod, B., Ludwig, R., Sillmann, J., 2021. Ten-year return levels of sub-daily extreme precipitation over Europe. Earth Syst. Sci. Data 13, 983–1003. https://doi.org/10.5194/essd-13-983-2021.
Prein, A.F., Rasmussen, R.M., Ikeda, K., Liu, C., Clark, M.P., Holland, G.J., 2017. The future intensification of hourly precipitation extremes. Nat. Clim. Chang. 7, 48–52. https://doi.org/10.1038/nclimate3168.
Rafiei-Sardooi, E., Azareh, A., Choubin, B., Mosavi, A.H., Clague, J.J., 2021. Evaluating urban flood risk using hybrid method of TOPSIS and machine learning. Int. J. Disaster Risk Reduct. 66, 102614. https://doi.org/10.1016/j.ijdrr.2021.102614.
Reimann, L., Koks, E., De Moel, H., Ton, M.J., Aerts, J.C.J.H., 2024. An empirical social vulnerability map for flood risk assessment at global scale ("GlobE-SoVI"). Earth's Future 12, e2023EF003895. https://doi.org/10.1029/2023EF003895.

Reisinger, A., Garschagen, M., Mach, K.J., Pathak, M., Poloczanska, E., van Aalst, M., Ruane, A.C., Hoden, M., Hurlber, M., Mintenbeck, K., Pedace, R., Rojas Corradi, M., Viner, D., Vera, C., Kreibiehl, S., O'Neill, B., Pörtner, H.-O., Sillmann, J., Jones, R., Ranasinghe, R., 2020. The Concept of Risk in the IPCC Sixth Assessment Report: A Summary of Cross-Working Group Discussions. Intergovernmental Panel on Climate Change, Geneva, Switzerland.

Restemeyer, B., Woltjer, J., Van Den Brink, M., 2015. A strategy-based framework for assessing the flood resilience of cities – a Hamburg case study. Plan. Theory Pract. 16, 45–62. https://doi.org/10.1080/14649357.2014.1000950.

Rose, J., Wilke, C.B., 2015. Climate Change Vulnerability in Cities: The Case of Hamburg.

Rosenzweig, B., Montalto, F.A., Orton, P., Kaatz, J., Maher, N., Kleyman, J., Chen, Z., Sanderson, E., Adhikari, N., McPhearson, T., Herreros-Cantis, P., 2024. NPCC4: climate change and new York City's flood risk. Ann. N. Y. Acad. Sci. 1539, 127–184. https://doi.org/10.1111/nyas.15175.

Ross, H., Shaw, S., Rissik, D., Cliffe, N., Chapman, S., Hounsell, V., Udy, J., Trinh, N.T., Schoeman, J., 2015. A participatory systems approach to understanding climate adaptation needs. Clim. Chang. 129, 27–42. https://doi.org/10.1007/s10584-014-1318-6.

Rossman, L.A., Simon, M.A., 2022. Storm water management model user's manual version 5.2 (user manual), EPA/600/R-22/030. United States Environmental Protection Agency (EPA), Center for Environmental Solutions and Emergency Response, Office of Research and Development, Cincinnati, OH 45268.

Rözer, V., Müller, M., Bubeck, P., Kienzler, S., Thieken, A., Pech, I., Schröter, K., Buchholz, O., Kreibich, H., 2016. Coping with pluvial floods by private households. Water 8, 304. https://doi.org/10.3390/w8070304.

Rözer, V., Peche, A., Berkhahn, S., Feng, Y., Fuchs, L., Graf, T., Haberlandt, U., Kreibich, H., Sämann, R., Sester, M., Shehu, B., Wahl, J., Neuweiler, I., 2021. Impact-based forecasting for pluvial floods. Earth's Future 9, 2020EF001851. https://doi.org/10.1029/2020EF001851.

Rufat, S., Tate, E., Emrich, C.T., Antolini, F., 2019. How valid are social vulnerability models? Ann. Am. Assoc. Geogr. 109, 1131–1153. https://doi.org/10.1080/24694452.2018.1535887.

Saaty, T.L., 1990. How to make a decision: the analytic hierarchy process. Eur. J. Oper. Res. 48, 9–26. https://doi.org/10.1016/0377-2217(90)90057-I.

Santos, V.M., Casas-Prat, M., Poschlod, B., Ragno, E., Van Den Hurk, B., Hao, Z., Kalmár, T., Zhu, L., Najafi, H., 2021. Statistical modelling and climate variability of compound surge and precipitation events in a managed water system: a case study in the Netherlands. Hydrol. Earth Syst. Sci. 25, 3595–3615. https://doi.org/10.5194/hess-25-3595-2021.

Santos, A.P., De Angeli, S., Hanf, F.S., Mirbach, C., Van Maanen, N., Benson, V., De Ruiter, M.C., Dunant, A., Terzi, S., Schweizer, P.-J., Nunes Carvalho, T.M., Madruga De Brito, M., De Polt, K., Šakić Trogrlić, R., Van Den Homberg, M., 2026. Workshop report—vulnerability in multi-hazard risks: addressing its complexity and dynamics. iScience 29 (4), 115250. https://doi.org/10.1016/j.isci.2026.115250.

Schanze, J., 2018. Pluvial flood risk management: an evolving and specific field. J. Flood Risk Manag. 11, 227–229. https://doi.org/10.1111/jfr3.12487.

Schmitt, T.G., Scheid, C., 2020. Evaluation and communication of pluvial flood risks in urban areas. WIREs Water 7, e1401. https://doi.org/10.1002/wat2.1401.

Shannon, C.E., 1948. A mathematical theory of communication. Bell Syst. Tech. J. 27, 379–423. https://doi.org/10.1002/j.1538-7305.1948.tb01338.x.

Shi, W., Tian, J., Zhang, J., Namaiti, A., He, W., Zhang, D., Zeng, J., 2026. Optimizing multidimensional land use for flood regulation supply-demand matching: evidence from a GWRF-SHAP model. J. Environ. Manag. 411, 130219. https://doi.org/10.1016/j.jenvman.2026.130219.

Sillmann, J., Raupach, T.H., Findell, K.L., Donat, M., Alves, L.M., Alexander, L., Borchert, L., De Amorim, P.B., Buontempo, C., Fischer, E.M., Franzke, C.L., Guan, B., Haasnoot, M., Hawkins, E., Jacob, D., Mahon, R., Maraun, D., Morrison, M.A., Poschlod, B., Ruane, A.C., Shampa, Stephenson, T., Van Der Wel, N., Wang, Z., Zhang, X., Županić, J., 2024. Climate extremes and risks: links between climate science and decision-making. Front. Clim. 6, 1499765. https://doi.org/10.3389/fclim.2024.1499765.

Skougaard Kaspersen, P., Høegh Ravn, N., Arnbjerg-Nielsen, K., Madsen, H., Drews, M., 2017. Comparison of the impacts of urban development and climate change on exposing European cities to pluvial flooding. Hydrol. Earth Syst. Sci. 21, 4131–4147. https://doi.org/10.5194/hess-21-4131-2017.

Stolte, T.R., Koks, E.E., de Moel, H., Reimann, L., van Vliet, J., de Ruiter, M.C., Ward, P.J., 2024. Vulneracity–drivers and dynamics of urban vulnerability based on a global systematic literature review. Int. J. Disaster Risk Reduct. 108, 104535. https://doi.org/10.1016/j.ijdrr.2024.104535.

Strange, K.F., March, H., Satorras, M., 2024. Incorporating climate justice into adaptation planning: the case of San Francisco. Cities 144, 104627. https://doi.org/10.1016/j.cities.2023.104627.

Swain, D.L., Wing, O.E.J., Bates, P.D., Done, J.M., Johnson, K.A., Cameron, D.R., 2020. Increased flood exposure due to climate change and population growth in the United States. Earth's Future 8, e2020EF001778. https://doi.org/10.1029/2020EF001778.

Teebken, J., 2024. Opportunities and limitations for social justice in Germany's climate adaptation policy. Z. Politwiss. 34, 231–253. https://doi.org/10.1007/s41358-024-00382-w.

Thieken, A.H., Bessel, T., Kienzler, S., Kreibich, H., Müller, M., Pisi, S., Schröter, K., 2016. The flood of June 2013 in Germany: how much do we know about its impacts? Nat. Hazards Earth Syst. Sci. 16, 1519–1540. https://doi.org/10.5194/nhess-16-1519-2016.

Usui, H., Teraki, A., Okunuki, K., Satoh, T., 2020. A comparison of neighbourhood relations based on ordinary Delaunay diagrams and area Delaunay diagrams: an application to define the neighbourhood relations of buildings. Int. J. Geogr. Inf. Sci. 34, 2177–2203. https://doi.org/10.1080/13658816.2020.1748191.

Van Ootegem, L., Verhofstadt, E., Van Herck, K., Creten, T., 2015. Multivariate pluvial flood damage models. Environ. Impact Assess. Rev. 54, 91–100. https://doi.org/10.1016/j.eiar.2015.05.005.

Veerkamp, C.J., Schipper, A.M., Hedlund, K., Lazarova, T., Nordin, A., Hanson, H.I., 2021. A review of studies assessing ecosystem services provided by urban green and blue infrastructure. Ecosyst. Serv. 52, 101367. https://doi.org/10.1016/j.ecoser.2021.101367.

Veleda, S., Martínez-Graña, A., Santos-Francés, F., Sánchez-SanRoman, J., Criado, M., 2017. Analysis of the hazard, vulnerability, and exposure to the risk of flooding (Alba de Yeltes, Salamanca, Spain). Appl. Sci. 7, 157. https://doi.org/10.3390/app7020157.

Vogelbacher, A., von Szombathely, M., Lennartz, M., Poschlod, B., Sillmann, J., 2026. A high-resolution framework for urban pluvial flood risk mapping. Nat. Hazards Earth Syst. Sci. (NHESS) 26, 2765–2783. https://doi.org/10.5194/nhess-26-2765-2026.

von Szombathely, M., Hanf, F.S., Bareis, J., Meier, L., Oßenbrügge, J., Pohl, T., 2023. An index-based approach to assess social vulnerability for Hamburg, Germany. Int. J. Disaster Risk Sci. 14, 782–794. https://doi.org/10.1007/s13753-023-00517-7.

Wahl, T., Jain, S., Bender, J., Meyers, S.D., Luther, M.E., 2015. Increasing risk of compound flooding from storm surge and rainfall for major US cities. Nat. Clim. Chang. 5, 1093–1097. https://doi.org/10.1038/nclimate2736.

Wamsler, C., 2017. Stakeholder involvement in strategic adaptation planning: transdisciplinarity and co-production at stake? Environ. Sci. Pol. 75, 148–157. https://doi.org/10.1016/j.envsci.2017.03.016.

Waser, J., Fuchs, R., Ribičić, H., Blöschl, G., 2011. Visuelle Aktionsplanung im Hochwassermanagement mit Visdom. Forum Für Hydrol. Wasserbewirtsch. 30, 280–286.

Wu, S., Zhou, X., Reyns, J., Yamazaki, D., Yin, J., Li, X., 2024. Climate change and urban sprawl: unveiling the escalating flood risks in river deltas with a deep dive into the GBM river delta. Sci. Total Environ. 947, 174703. https://doi.org/10.1016/j.scitotenv.2024.174703.

Yang, L., Hoffmann, P., Scheffran, J., Rühe, S., Fischereit, J., Gasser, I., 2018a. An agent-based modeling framework for simulating human exposure to environmental stresses in urban areas. Urban Sci. 2, 36. https://doi.org/10.3390/urbansci2020036.

Yang, W., Xu, K., Lian, J., Ma, C., Bin, L., 2018b. Integrated flood vulnerability assessment approach based on TOPSIS and Shannon entropy methods. Ecol. Indic. 89, 269–280. https://doi.org/10.1016/j.ecolind.2018.02.015.